RESEARCH ARTICLE | SEPTEMBER 24 2025

Hirota condition analysis of N-solitons and their derived waves for a nonlocal (2 + 1)-dimensional modified Kadomtsev–Petviashvili equation

Litao Gai (盖立涛); Wen-Xiu Ma (马文秀); Lianbao Jin (金连宝)

Physics of Fluids 37, 097172 (2025)
https://doi.org/10.1063/5.0288755

Hirota condition analysis of N-solitons and their derived waves for a nonlocal (2 + 1)-dimensional modified Kadomtsev–Petviashvili equation

Cite as: Phys. Fluids 37, 097172 (2025); doi: 10.1063/5.0288755
Submitted: 2 July 2025 · Accepted: 9 September 2025 ·
Published Online: 24 September 2025

View Online Export Citation CrossMark

Litao Gai (盖立涛),[1,a] Wen-Xiu Ma (马文秀),[1,2,3,4,a] and Lianbao Jin (金连宝)[5,a]

AFFILIATIONS

[1]School of Mathematical Sciences, Zhejiang Normal University, Jinhua 321004, Zhejiang, China
[2]Department of Mathematics, King Abdulaziz University, Jeddah 21589, Saudi Arabia
[3]Department of Mathematics and Statistics, University of South Florida, Tampa, Florida 33620-5700, USA
[4]Material Science Innovation and Modelling, Department of Mathematical Sciences, North-West University, Mafikeng Campus, Mmabatho 2735, South Africa
[5]School of Basic Medical sciences, Shandong Second Medical University, Weifang 261053, Shandong, China

[a]Authors to whom correspondence should be addressed: litaogai@zjnu.edu.cn; mawx@cas.usf.edu; and jinlianbao@sdsmu.edu.cn

ABSTRACT

This article mainly studies the Hirota condition analysis and a series of multi-wave solutions of a nonlocal $(2+1)$-dimensional modified Kadomtsev–Petviashvili equation. The Hirota bilinear form is given under integrability conditions, which provide a prerequisite for obtaining N-soliton solutions. Moreover, by performing specific constraints on the Hirota condition of N-solitons, some novel and interesting multi-wave solutions with fully elastic structures can be further generated. Particularly, based on a type of new test function with a multi-layer network structure, one class of meshy-periodic lump wave solution is obtained using the bilinear neural network method. The three-dimensional dynamics of all results obtained are conducive to revealing nonlinear interaction phenomena of shallow-water waves.

I. INTRODUCTION

Up to now, the soliton solutions of integrable nonlinear evolution equations have always been a focus of research in nonlinear science. Solitons have significant applications in natural phenomena such as matter-wave.[1–4] However, among many integrable nonlinear mathematical and physical equations, those with N-soliton solutions are extremely rare. The most representative equations with N-soliton solutions mainly include the well-known KdV equation,[5–9] as well as the classical nonlinear Schrödinger equation,[10–15] the Kadomtsev–Petviashvili equation,[16,17] the sine-Gordon equation,[18] the $(2+1)$-dimensional Sawada–Kotera equation,[19] the integrable combined fractional higher-order mKdV equation,[20] and so on.[21–24]

Integrable nonlinear evolution equations can be used to describe some novel nonlinear phenomena when considering the shape and collision effects of fluids.[25–27] Describing the interaction of shallow-water waves in the ocean, a nonlocal integrable system in $(2+1)$-dimensions with fifth-order linear dispersion and third power nonlinear disturbance factors will be considered in this paper. Namely, a nonlocal $(2+1)$-dimensional mKP equation as follows

$$u_t + \alpha u_{xxx} + \alpha_1 u u_x + \beta u_{5x} + \beta_1 (u_x u_{xx} + u u_{xxx}) + \beta_2 u^2 u_x + \gamma \int u_{yy} \mathrm{d}x = 0, \tag{1}$$

where α, α_1, β, β_1, β_2, and γ are non-zero constants. Easy to see that Eq. (1) has multiple nonlinear factors and is a new shallow-water wave model like the KP equation, in a nonlocal environment with multi-parameters. If $\beta = \beta_1 = \beta_2 = 0$ and Eq. (1) takes a first-order partial derivative of x, it can degenerate into

$$(u_t + \alpha u_{xxx} + \alpha_1 u u_x)_x + \gamma u_{yy} = 0, \tag{2}$$

as we can see that Eq. (2) is the standard $(2+1)$-dimensional Kadomtsev–Petviashvili equation.[28,29] When $\alpha_1 = 6\alpha$, the classic Eq. (2) is Lax integrable. In particular, Lou uses $\hat{P}$-$\hat{T}$-$\hat{C}$ symmetry reduction to give a new integrable form of Eq. (2) with Lax pair, called the ABKP system.[30] The partial-rogue ripple solutions based on Wronskian determinant of a nonlocal ABKP system are obtained by Cao *et al.*[31] Ma provided a proof that the $(3+1)$-dimensional bilinear

KP equation, a generalization of Eq. (2) in $(3+1)$-dimensions, does not satisfy the Hirota 3-soliton condition.[32]

There are many studies on Eq. (2), and we will not list them one by one here. An issue of great theoretical and applied value is that, we can further explore the N-soliton solutions and novel shallow-water wave interaction characteristics of Eq. (1) under certain specific conditions, based on the integrability of Eq. (2). To our knowledge, the current research on Eq. (1) is relatively rare, and the applications of many exact analytical methods to Eq. (1) still requires further study. Such as the Darboux transformation method,[15,16] the trilinear method,[22] the Hirota bilinear method,[19,21,23,33–36] and Painlevé analysis method[37,38] for Eq. (1) have not been given.

In this work, we will construct abundant new exact traveling wave solutions which are used to describe the interaction phenomena of shallow-water waves based on the integrable form of Eq. (1), including N-soliton solutions, multi-breather wave solutions, multi-lump wave solutions, mixed-type multi-wave solutions, and a new type of meshy-periodic lump wave solutions. The dynamics of all the multi-wave solutions presented and evolution phenomena of some nonlinear elastic collisions will be well demonstrated through 3D and 2D graphs. These new solutions will fully demonstrate that Eq. (1) can be used to reveal or describe nonlinear wave propagation phenomena. It is worth mentioning that applying neural network technology to construct exact solutions of integrable nonlinear equations has become a popular research topic in recent years, and this article will also utilize this new idea.[39–41]

The organizational structure of this paper is as follows. In Sec. II, we will provide the bilinear form of Eq. (1) using the Hirota method based on the Bell polynomial theory of integrable equations. Section III presents a standard form of N-soliton solutions, based on the Hirota bilinear form of Eq. (1). In Sec. IV, the multi-breather waves of Eq. (1) will be presented using the Hirota condition of N-solitons. We also give the multi-lump waves and hybrid waves in Secs. V and VI, respectively. Section VII provides a new class of meshy-periodic lump waves through a test function with multi-layer neural network structure in BNNM. In Sec. VIII, we make some conclusions.

II. HIROTA BILINEAR FORM

According to the integrability condition of Eq. (2), we know that Eq. (1) cannot guarantee complete integrability under any conditions. However, when the coefficients satisfy a specific conservation relationship, Eq. (1) is integrable. Similarly, when the parameters satisfy $\alpha_1 = 6\alpha$ and $\beta_2 = 3\beta_1 = 45\beta$, Eq. (1) corresponds to a nonlocal integrable form as follows

$$\begin{aligned} &u_t + \alpha u_{xxx} + 6\alpha u u_x + \beta u_{5x} + 15\beta(u_x u_{xx} + u u_{xxx}) \\ &\quad + 45\beta u^2 u_x + \gamma \int u_{yy} \mathrm{d}x = 0, \end{aligned} \tag{3}$$

where α, β, and γ are arbitrary non-zero real constants. In order to obtain a bilinear form for Eq. (1), let's start with the following second-order logarithmic transformation, that is,

$$u = \xi_x = \mu_{xx} = 2(\ln\phi)_{xx}, \quad \phi > 0, \tag{4}$$

where $\xi = \xi(x,y,t)$, $\mu = \mu(x,y,t)$, and $\phi = \phi(x,y,t)$ are functions of variables x, y, and t. By taking $u = \xi_x$, the nonlocal Eq. (3) can be written as

$$\begin{aligned} &\xi_{xt} + \alpha\xi_{xxxx} + 6\alpha\xi_x\xi_{xx} + \beta\xi_{6x} + 15\beta(\xi_{xx}\xi_{xxx} + \xi_x\xi_{xxxx}) \\ &\quad + 45\beta\xi_x^2\xi_{xx} + \gamma\xi_{yy} = 0, \end{aligned} \tag{5}$$

then, further substituting $\xi = \mu_x$ into Eq. (5) and integrating the variable x once, which reads

$$\begin{aligned} &\int(\mu_{xxt} + \alpha\mu_{5x} + 6\alpha\mu_{xx}\mu_{xxx} + \beta\mu_{7x} + 15\beta(\mu_{xxx}\mu_{xxxx} + \mu_{xx}\mu_{5x}) \\ &\quad + 45\beta\mu_{xx}^2\mu_{xxx} + \gamma\mu_{xyy})\mathrm{d}x = 0, \end{aligned} \tag{6}$$

by setting the integral constant of Eq. (6) to zero, we have

$$\mu_{xt} + \alpha\mu_{xxxx} + 3\alpha\mu_{xx}^2 + \beta\mu_{6x} + 15\beta\mu_{xx}\mu_{xxxx} + 15\beta\mu_{xx}^3 + \gamma\mu_{yy} = 0. \tag{7}$$

Finally, let $\mu = 2\ln\phi$ can transform Eq. (7) into the new form, as follows:

$$\begin{aligned} &\frac{2}{\phi^2}\left[\alpha\phi\left(\frac{\partial^4\phi}{\partial x^4}\right) - 4\alpha\left(\frac{\partial\phi}{\partial x}\right)\left(\frac{\partial^3\phi}{\partial x^3}\right) + 3\alpha\left(\frac{\partial^2\phi}{\partial x^2}\right)^2 + \beta\phi\left(\frac{\partial^6\phi}{\partial x^6}\right)\right. \\ &\quad - 6\beta\left(\frac{\partial^5\phi}{\partial x^5}\right)\left(\frac{\partial\phi}{\partial x}\right) + 15\beta\left(\frac{\partial^4\phi}{\partial x^4}\right)\left(\frac{\partial^2\phi}{\partial x^2}\right) - 10\beta\left(\frac{\partial^3\phi}{\partial x^3}\right)^2 \\ &\quad \left. + \phi\left(\frac{\partial^2\phi}{\partial t\partial x}\right) - \left(\frac{\partial\phi}{\partial t}\right)\left(\frac{\partial\phi}{\partial x}\right) + \eta\phi\left(\frac{\partial^2\phi}{\partial y^2}\right) - \eta\left(\frac{\partial\phi}{\partial y}\right)^2\right] = 0, \end{aligned} \tag{8}$$

where $\phi = \phi(x,y,t) > 0$. Eliminating the denominator, Eq. (8) can be simplified into a bilinear form to Eq. (1), namely,

$$\begin{aligned} \mathrm{B_{mKP}}(\phi) \triangleq\, &\alpha(\phi\phi_{xxxx} - 4\phi_x\phi_{xxx} + 3\phi_{xx}^2) \\ &+ \beta(\phi\phi_{6x} - 6\phi_x\phi_{5x} + 15\phi_{xx}\phi_{xxxx} - 10\phi_{xxx}^2) \\ &+ \phi\phi_{xt} - \phi_x\phi_t + \gamma\phi\phi_{yy} - \gamma\phi_y^2 = 0. \end{aligned} \tag{9}$$

Remark 2.1 Based on the Bell polynomial theory of integrable bilinear equations,[42] Eq. (9) corresponds to a Hirota bilinear (HB) form as below

$$\mathrm{HB_{mKP}}(\phi) \triangleq (\alpha D_x^4 + \beta D_x^6 + D_x D_t + \gamma D_y^2)\phi\cdot\phi = 0, \tag{10}$$

where D_t, D_x, and D_y are Hirota derivatives, defined by[19,33–36]

$$\begin{aligned} D_x^K D_y^P D_t^L(\phi\cdot\psi) = &\left(\frac{\partial}{\partial x} - \frac{\partial}{\partial\tilde{x}}\right)^K \left(\frac{\partial}{\partial y} - \frac{\partial}{\partial\tilde{y}}\right)^P \left(\frac{\partial}{\partial t} - \frac{\partial}{\partial\tilde{t}}\right)^L \phi(x,y,t) \\ &\cdot\psi(\tilde{x},\tilde{y},\tilde{t})|_{\tilde{x}=x,\tilde{y}=y,\tilde{t}=t}. \end{aligned}$$

III. HIROTA CONDITION OF N-SOLITONS

In this section, the Hirota method[19,21–23] is used to analyze the standard condition of N-soliton solutions of Eq. (1). In order to provide general form of the N-solitons for Eq. (1), we will introduce the following standardized theorem.

Theorem 1. *Based on* $\mathrm{HB_{mKP}}$ Eq. (10) via $\gamma = -10\beta$, *the nonlocal* Eq. (1) *with integrability condition has the following standard form of* N*-solitons*

$$u_N = 2\frac{\partial^2}{\partial x^2}\ln(\phi_N), \quad N = 1,2,3,\ldots, \tag{11}$$

where ϕ_N satisfies the Hirota condition, as follows:

$$\begin{cases} \phi_N = 1 + \sum_{\rho_i=0,1} \exp\left(\sum_{1\le i<j}^{N} \rho_i\rho_j\theta_{ij} + \sum_{i=1}^{N}\rho_i\xi_i\right), \\ \xi_i = \delta_i x - \delta_i^3 y + \left(9\beta\delta_i^5 - \alpha\delta_i^3\right)t + \xi_i^{(0)}, \\ e^{\theta_{ij}} = \dfrac{\left(5\beta\left(\delta_i^2+\delta_i\delta_j+\delta_j^2\right)+\alpha\right)\left(\delta_i-\delta_j\right)^2}{\left(5\beta\left(\delta_i^2-\delta_i\delta_j+\delta_j^2\right)+\alpha\right)\left(\delta_i+\delta_j\right)^2}, \quad 1\le i<j\le N\in N^*. \end{cases} \tag{12}$$

Proof. Before proving standard condition (12) it is necessary to first explain that Eq. (11) can be expressed as a solution to Eq. (1). This can actually be attributed to the direct relationship between Eq. (1) and bilinear forms (9) or (10) under the integrability conditions $\alpha_1 = 6\alpha$ and $\beta_2 = 3\beta_1 = 45\beta$, as follows

$$P_{\mathrm{mKP}}(u) \equiv \left[\frac{2B_{\mathrm{mKP}}(\phi)}{\phi^2}\right]_{xx} = \left[\frac{2HB_{\mathrm{mKP}}(\phi)}{\phi^2}\right]_{xx}, \tag{13}$$

therefore, when ϕ is a solution to Eqs. (9) or (10) Eq. (11) must be a solution to Eq. (1).

Now, we expand the function ϕ in Eq. (10) into a power series of ϱ, which becomes

$$\phi \triangleq \phi_N = 1 + \sum_{k=1}^{N}\phi^{(k)}\varrho^k, \quad N\in N^*, \tag{14}$$

substituting Eq. (14) into Eq. (10) with $\gamma = -10\beta$ and collect the coefficients of ϱ^k to the same power, that is,

$$o(\varrho^1)\ 2\left(\alpha\partial_x^4 + \beta\partial_x^6 + \partial_x\partial_t - 10\beta\partial_y^2\right)\phi^{(1)} = 0, \tag{15}$$

$$\begin{aligned} o(\varrho^2)\ & 2(\alpha\partial_x^4 + \beta\partial_x^6 + \partial_x\partial_t - 10\beta\partial_y^2)\phi^{(2)} \\ & = -(\alpha D_x^4 + \beta D_x^6 + D_xD_t - 10\beta D_y^2)\phi^{(1)}\cdot\phi^{(1)}, \end{aligned} \tag{16}$$

$$\begin{aligned} o(\varrho^3)\ & 2(\alpha\partial_x^4 + \beta\partial_x^6 + \partial_x\partial_t - 10\beta\partial_y^2)\phi^{(3)} \\ & = -2(\alpha D_x^4 + \beta D_x^6 + D_xD_t - 10\beta D_y^2)\phi^{(1)}\cdot\phi^{(2)}, \\ & \cdots \end{aligned} \tag{17}$$

To obtain $\phi^{(k)}(k=1,2,\ldots,N)$, we assume that $\phi^{(1)}$ in Eq. (15) has a general solution of the following form:

$$\phi^{(1)} = \sum_{i=1}^{n} e^{\xi_i},\ \xi_i = \delta_i x + \omega_i y + \nu_i t + \xi_i^{(0)}, \quad i=1,2,\ldots,n, \tag{18}$$

where δ_i, ω_i, ν_i, and $\xi_i^{(0)}$ are undetermined arbitrary constants. Then, we substitute Eq. (18) into Eq. (15) for calculation, and a set of parameter solutions can be obtained, that is,

$$\delta_i = \delta_i, \quad \omega_i = -\delta_i^3, \quad \nu_i = 9\beta\delta_i^5 - \alpha\delta_i^3, \quad \xi_i^{(0)} = \xi_i^{(0)}. \tag{19}$$

(i) If $n = 1$, Eq. (18) is written as

$$\phi^{(1)} = e^{\xi_1}, \quad \xi_1 = \delta_1 x - \delta_1^3 y + (9\beta\delta_1^5 - \alpha\delta_1^3)t + \xi_1^{(0)}, \tag{20}$$

substitute Eq. (20) into Eq. (16) yields $2(\alpha\partial_x^4 + \beta\partial_x^6 + \partial_x\partial_t - 10\beta\partial_y^2)\phi^{(2)} = 0$, so we make $\phi^{(2)} = 0$ and thereby promoting $\phi^{(j)} = 0(j=3,4,\ldots,N)$. By selecting $\varrho = 1$, Eq. (14) is truncated into the following form

$$\phi_1 = 1 + e^{\xi_1},\ \xi_1 = \delta_1 x - \delta_1^3 y + (9\beta\delta_1^5 - \alpha\delta_1^3)t + \xi_1^{(0)}, \tag{21}$$

which satisfies the standard condition (12) According to the relationship between u and ϕ in Eq. (13), we obtain a 1-soliton of Eq. (1), namely,

$$u_1 = 2\ln(\phi_1)_{xx} = \frac{2\delta_1^2 e^{\xi_1}\left(\phi_1 - e^{\xi_1}\right)}{\phi_1^2}. \tag{22}$$

(ii) If $n = 2$, then Eq. (18) becomes

$$\begin{cases} \phi^{(1)} = e^{\xi_1} + e^{\xi_2}, \\ \xi_1 = \delta_1 x - \delta_1^3 y + (9\beta\delta_1^5 - \alpha\delta_1^3)t + \xi_1^{(0)}, \\ \xi_2 = \delta_2 x - \delta_2^3 y + (9\beta\delta_2^5 - \alpha\delta_2^3)t + \xi_2^{(0)}, \end{cases} \tag{23}$$

by substituting Eq. (23) into Eq. (16) and organizing it, we can obtain

$$\begin{aligned} & (\alpha\partial_x^4 + \beta\partial_x^6 + \partial_x\partial_t - 10\beta\partial_y^2)\phi^{(2)} \\ & \quad = 3\delta_1\delta_2(\delta_1-\delta_2)^2(5\beta(\delta_1^2+\delta_1\delta_2+\delta_2^2)+\alpha)e^{\xi_1+\xi_2}, \end{aligned} \tag{24}$$

by solving Eq. (24), we can easily obtain a specific solution for $\phi^{(2)}$, as follows:

$$\phi^{(2)} = e^{\xi_1+\xi_2+\theta_{12}}, \quad e^{\theta_{12}} = \frac{(5\beta(\delta_1^2+\delta_1\delta_2+\delta_2^2)+\alpha)(\delta_1-\delta_2)^2}{(5\beta(\delta_1^2-\delta_1\delta_2+\delta_2^2)+\alpha)(\delta_1+\delta_2)^2}. \tag{25}$$

Next, we substitute Eqs. (23) and (25) together into Eq. (17) for expansion. After organizing the substituted Eq. (17), it can be concluded that there are only the following two results on the right side of the equal sign, namely

$$\begin{aligned} & -(\alpha D_x^4 + \beta D_x^6 + D_xD_t - 10\beta D_y^2)e^{\xi_1}\cdot e^{\xi_1+\xi_2+\theta_{12}} \\ & \quad = \left[\alpha(-\delta_2)^4 + \beta(-\delta_2)^6 + (-\delta_2)(\alpha\delta_2^3 - 9\beta\delta_2^5) - 10\beta(\delta_2^3)^2\right] \\ & \qquad \times e^{2\xi_1+\xi_2+\theta_{12}} = 0, \\ & -(\alpha D_x^4 + \beta D_x^6 + D_xD_t - 10\beta D_y^2)e^{\xi_2}\cdot e^{\xi_1+\xi_2+\theta_{12}} \\ & \quad = \left[\alpha(-\delta_1)^4 + \beta(-\delta_1)^6 + (-\delta_1)(\alpha\delta_1^3 - 9\beta\delta_1^5) - 10\beta(\delta_1^3)^2\right] \\ & \qquad \times e^{\xi_1+2\xi_2+\theta_{12}} = 0, \end{aligned} \tag{26}$$

thus, we also make $\phi^{(3)} = 0$ and thereby promote $\phi^{(j)} = 0(j=4,5,\ldots,N)$. By selecting $\varrho = 1$, Eq. (14) will be truncated into a new form, that is,

$$\begin{aligned} & \phi_2 = 1 + e^{\xi_1} + e^{\xi_2} + e^{\xi_1+\xi_2+\theta_{12}}, \\ & e^{\theta_{12}} = \frac{(5\beta(\delta_1^2+\delta_1\delta_2+\delta_2^2)+\alpha)(\delta_1-\delta_2)^2}{(5\beta(\delta_1^2-\delta_1\delta_2+\delta_2^2)+\alpha)(\delta_1+\delta_2)^2}, \end{aligned} \tag{27}$$

which also satisfies the standard condition (12) Then, a 2-soliton for Eq. (1) can be presented below

$$u_2 = 2\ln(\phi_2)_{xx} = \frac{2\varrho}{\phi_2^2}\Big(-\varrho^3(\delta_1+\delta_2)^2 e^{2\xi_1+2\xi_2+2\theta_{12}} - 2\varrho^2\delta_2(\delta_1+\delta_2)e^{\xi_1+2\xi_2+\theta_{12}} - 2\varrho^2\delta_1(\delta_1+\delta_2)e^{2\xi_1+\xi_2+\theta_{12}} + \phi_2\varrho(\delta_1+\delta_2)^2 e^{\xi_1+\xi_2+\theta_{12}} - 2e^{\xi_1+\xi_2}\varrho\delta_1\delta_2 - e^{2\xi_1}\varrho\delta_1^2 - e^{2\xi_2}\varrho\delta_2^2 + \phi_2\left(\delta_1^2 e^{\xi_1}+\delta_2^2 e^{\xi_2}\right)\Big). \tag{28}$$

(iii) If $n=3$, Eq. (18) has the following third form:

$$\begin{cases} \phi^{(1)} = e^{\xi_1}+e^{\xi_2}+e^{\xi_3}, \\ \xi_1 = \delta_1 x - \delta_1^3 y + (9\beta\delta_1^5 - \alpha\delta_1^3)t + \xi_1^{(0)}, \\ \xi_2 = \delta_2 x - \delta_2^3 y + (9\beta\delta_2^5 - \alpha\delta_2^3)t + \xi_2^{(0)}, \\ \xi_3 = \delta_3 x - \delta_3^3 y + (9\beta\delta_3^5 - \alpha\delta_3^3)t + \xi_3^{(0)}, \end{cases} \tag{29}$$

substituting Eq. (29) into Eq. (16) and calculating it, we still get a specific solution for $\phi^{(2)}$ in the same way, that is,

$$\phi^{(2)} = e^{\xi_1+\xi_2+\theta_{12}} + e^{\xi_1+\xi_3+\theta_{13}} + e^{\xi_2+\xi_3+\theta_{23}}, \quad e^{\theta_{ij}} = \frac{(5\beta(\delta_i^2+\delta_i\delta_j+\delta_j^2)+\alpha)(\delta_i-\delta_j)^2}{(5\beta(\delta_i^2-\delta_i\delta_j+\delta_j^2)+\alpha)(\delta_i+\delta_j)^2}, \tag{30}$$

then, we substitute Eqs. (29) and (30) together into Eq. (17), which is simplified into the form as below

$$\begin{aligned}(\alpha\partial_x^4+\beta\partial_x^6+\partial_x\partial_t-10\beta\partial_y^2)\phi^{(3)} &= -(\alpha D_x^4+\beta D_x^6+D_xD_t-10\beta D_y^2)\sum_{i=1,i\neq j<k}^{3} e^{\xi_i}\cdot e^{\xi_j+\xi_k+\theta_{jk}} \\ &= -(\zeta_{1,23}+\zeta_{2,13}+\zeta_{3,12})e^{\xi_1+\xi_2+\xi_3},\end{aligned} \tag{31}$$

where $\zeta_{i,jk}$ $(i,j,k=1,\,2,\,3)$ satisfies one standard form, namely

$$\zeta_{i,jk} = \Big[\alpha(\delta_i-\delta_j-\delta_k)^4+\beta(\delta_i-\delta_j-\delta_k)^6 + (\delta_i-\delta_j-\delta_k)((9\beta\delta_j^5-\alpha\delta_j^3)+(9\beta\delta_k^5-\alpha\delta_k^3) - (9\beta\delta_i^5-\alpha\delta_i^3)) - 10\beta(\delta_j^3+\delta_k^3-\delta_i^3)^2\Big]e^{\theta_{jk}}, \quad j<k, \tag{32}$$

by combining Eqs. (31) and (32) for calculation, a specific solution for $\phi^{(3)}$ is obtained as follows

$$\phi^{(3)} = e^{\xi_1+\xi_2+\xi_3+\theta_{12}+\theta_{13}+\theta_{23}}, \quad e^{\theta_{ij}} = \frac{(5\beta(\delta_i^2+\delta_i\delta_j+\delta_j^2)+\alpha)(\delta_i-\delta_j)^2}{(5\beta(\delta_i^2-\delta_i\delta_j+\delta_j^2)+\alpha)(\delta_i+\delta_j)^2}, \quad 1\le i<j\le 3. \tag{33}$$

Now, we substitute Eqs. (29), (30), and (33) together into the equation via $o(\varrho^4)$, which can makes $(\alpha\partial_x^4+\beta\partial_x^6+\partial_x\partial_t-10\beta\partial_y^2)\phi^{(4)}=0$. Therefore, we still make $\phi^{(4)}=0$ and thereby promoting $\phi^{(j)}=0 (j=5,6,\ldots,N)$. By setting $\varrho=1$, Eq. (14) can be truncated into one form, that is,

$$\phi_3 = 1+e^{\xi_1}+e^{\xi_2}+e^{\xi_3}+e^{\xi_1+\xi_2+\theta_{12}}+e^{\xi_1+\xi_3+\theta_{13}} + e^{\xi_2+\xi_3+\theta_{23}}+e^{\xi_1+\xi_2+\xi_3+\theta_{12}+\theta_{13}+\theta_{23}}, \tag{34}$$

which still satisfies the standard condition (12) Then, a 3-soliton of Eq. (1) can be presented below

$$u_3 = 2\ln(\phi_3)_{xx} = \text{Omit}. \tag{35}$$

After our verification, the multi-soliton solutions of Eq. (1) for $n=4,5,6\ldots$ could be constructed in a similar way. Thus, when $n=N$, we can obtain the N-solitons with the standard condition (12) of nonlocal Eq. (1). □

Remark 3.1 By setting parameter values of $\alpha=\beta=1$, $\delta_1=0.2$, $\xi_1^{(0)}=1$ and $y=-x$, Figs. 1(a) and 1(d) show the dynamics of 1-soliton u_1 via Eq. (22).

Remark 3.2 By setting parameter values of $\alpha=\beta=1$, $\delta_1=0.4$, $\delta_2=-0.8$, $\xi_1^{(0)}=\xi_2^{(0)}=0$ and $y=-x$, Figs. 1(b) and 1(e) show the dynamics of 2-soliton u_2 via Eq. (28).

Remark 3.3 By setting parameter values of $\alpha=\beta=1$, $\varrho=1$, $\delta_1=0.6$, $\delta_2=-0.8$, $\delta_3=0.4$, $\xi_j^{(0)}=0 (j=1,\,2,\,3)$ and $y=-x$, Figs. 1(c) and 1(f) show the dynamics of 3-soliton u_3 via Eq. (35).

When a nonlinear system meets the condition of integrability, the soliton solutions it obtains (like the KdV equation[5–9]) will be highly stable. Therefore, after multi-solitons collide, each maintains its original amplitude, energy and propagation direction. It is easy to see from (b), (c), (e), and (f) in Fig. 1 that when multi-solitons collide, they each maintain strong stability. Under the influence of nonlinear effects, multi-solitons only experience a phase shift at the collision point, and the amplitude near that point decreases. The nonlinear characteristics of solitons have significant application value in shallow-water wave analysis and elastic systems, which can be applied in fields such as tsunami wave propagation prediction, ship fluid design, and offshore platform safety analysis.

IV. MULTI-BREATHER WAVES

When we impose some special constraints on the standard condition (12) the N-soliton solutions determined by expansion Eq. (11) can derive some peculiar and interesting multi-wave solutions. In this section, we will construct the multi-breather wave solutions of Eq. (1). Now, we need to impose the following constraints on condition (12) that is,

$$\delta_{2m-1} = \delta_{2m}^* \triangleq p_m + iq_m, \quad \xi_{2m-1}^{(0)} = \xi_{2m}^{(0)} = 0, \quad m=1,2,\ldots, \tag{36}$$

then Eq. (12) with the Hirota condition is rewritten as a new form by substituting Eq. (36) back into it, reads

$$\begin{cases} \phi_{2m} = 1+\sum_{\rho_i=0,1}\exp\left(\sum_{1\le i<j}^{2m}\rho_i\rho_j\theta_{ij}+\sum_{i=1}^{2m}\rho_i\xi_i\right), \\ \xi_{2m-1} = \xi_{2m}^* \triangleq \text{Re.}(\xi_{2m-1})+\text{Im.}(\xi_{2m-1})i = R_m + I_m i, \\ R_m = p_m x + p_m(3q_m^2-p_m^2)y \\ \quad +p_m\left[(9\beta p_m^2-\alpha)p_m^2+3(\alpha-30\beta p_m^2+15\beta q_m^2)q_m^2\right]t, \\ I_m = q_m x + q_m(q_m^2-3p_m^2)y \\ \quad +q_m\left[(9\beta q_m^2+\alpha)q_m^2-3(\alpha+30\beta q_m^2-15\beta p_m^2)p_m^2\right]t, \end{cases} \tag{37}$$

and

$$\lambda_{ij} \triangleq e^{\theta_{ij}} = \frac{(15\beta p_m^2-5\beta q_m^2+\alpha)q_m^2}{(15\beta q_m^2-5\beta p_m^2-\alpha)p_m^2} > 0, \quad \forall m\in N^*. \tag{38}$$

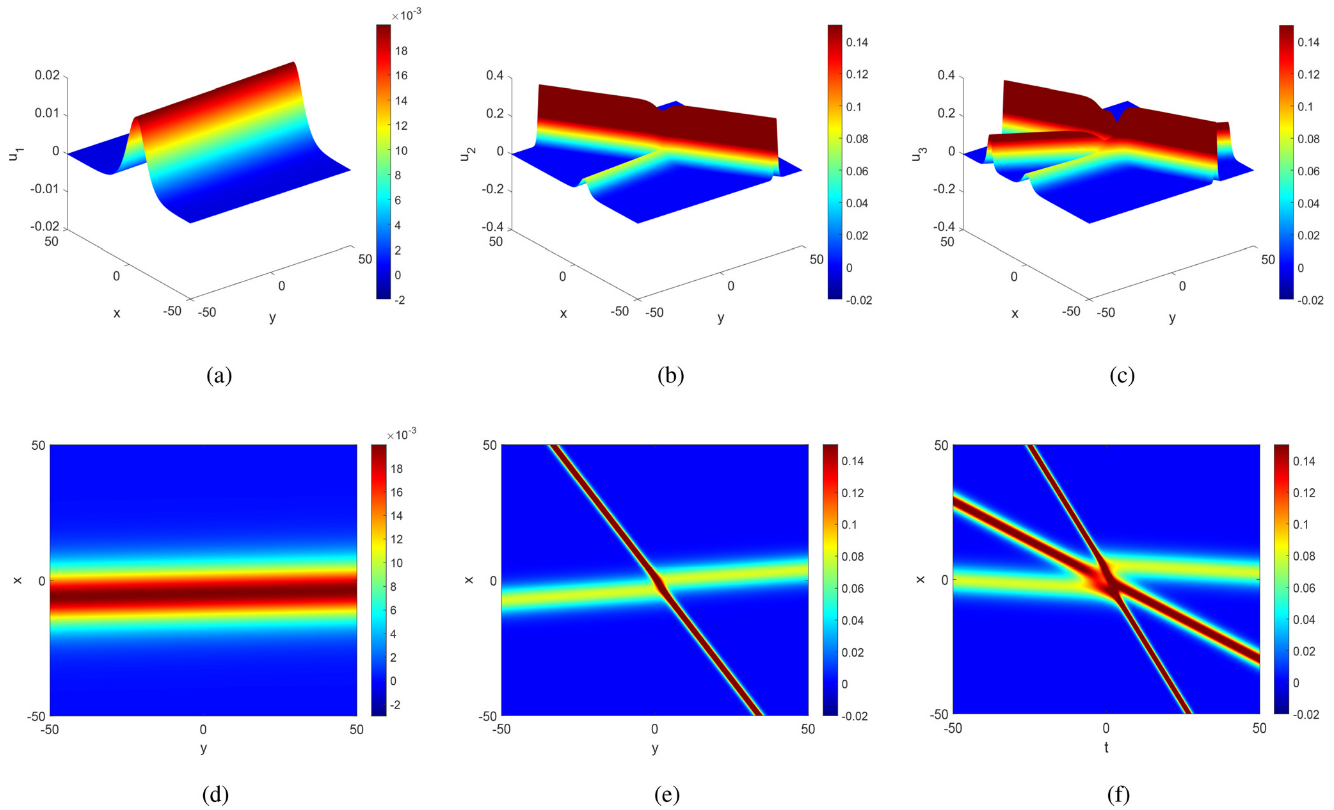

FIG. 1. The elastic collision phenomena among multi-solitons: 3D (top) and density (bottom) plots of $u_i (i = 1, 2, 3)$. (a) and (d) 1-soliton via (22); (b) and (e) 2-soliton via (28); and (c) and (f) 3-soliton via (35).

It should be noted that if $\phi_{2m} > 0$ is made in condition (35) $\lambda_{ij} > 0$ must be established. If all the above conditions are met, the multi-breather solutions can be generated based on Eq. (11), as follows

$$u_{2m}^{|M|} = 2\ln(\phi_{2m})_{xx}, \quad M = m. \tag{39}$$

Case (i). When $M = m = 1$, the first-order breather $u_2^{|1|}$ is presented via Eq. (39), which corresponds to the following condition

$$\phi_2 = 1 + e^{\xi_1} + e^{\xi_2} + \lambda_{12} e^{\xi_1 + \xi_2}, \tag{40}$$

where $\xi_i (i = 1, 2)$ and λ_{12} are given in Eqs. (37) and (38). The wave dynamics of $u_2^{|1|}$ with condition (40) will be shown by Remark 4.1.

Case (ii). When $M = m = 2$, the second-order breather $u_4^{|2|}$ is presented via Eq. (39), which corresponds to a condition as below

$$\phi_4 = 1 + \sum_{i=1}^{4} e^{\xi_i} + \sum_{1 \le i < j \le 4} \lambda_{ij} \cdot e^{\xi_i + \xi_j} + \sum_{1 \le i < j < k \le 4} \lambda_{ij}\lambda_{ik}\lambda_{jk} \cdot e^{\xi_i + \xi_j + \xi_k} + \prod_{1 \le i < j \le 4} \lambda_{ij} \cdot e^{\left(\sum_{i=1}^{4} \xi_i\right)}, \tag{41}$$

where $\xi_i (i = 1, 2, 3, 4)$ and $\lambda_{ij} (1 \le i < j \le 4)$ satisfy the Eqs. (37) and (38). The wave dynamics of $u_4^{|2|}$ with condition (41) are shown by Remark 4.2.

Case (iii). When $M = m = 3$, the third-order breather $u_6^{|3|}$ is presented via Eq. (39), which corresponds to the third condition, that is,

$$\begin{aligned}\phi_6 = {} & 1 + \sum_{i=1}^{6} e^{\xi_i} + \sum_{1 \le i < j \le 6} \lambda_{ij} \cdot e^{\xi_i + \xi_j} + \sum_{1 \le i < j < k \le 6} \lambda_{ij}\lambda_{ik}\lambda_{jk} \cdot e^{\xi_i + \xi_j + \xi_k} \\ & + \prod_{1 \le i < j \le 6} \lambda_{ij} \cdot e^{\left(\sum_{i=1}^{6} \xi_i\right)} + \sum_{1 \le i < j < k < l \le 6} \lambda_{ij}\lambda_{ik}\lambda_{jk}\lambda_{kl} \cdot e^{\xi_i + \xi_j + \xi_k + \xi_l} \\ & + \sum_{1 \le i < j < k < l < m \le 6} \lambda_{ij}\lambda_{ik}\lambda_{jk}\lambda_{kl}\lambda_{lm} \cdot e^{\xi_i + \xi_j + \xi_k + \xi_l + \xi_m},\end{aligned} \tag{42}$$

where $\xi_i (i = 1, 2, \ldots, 6)$ and $\lambda_{ij} (1 \le i < j \le 6)$ also satisfy the Eqs. (37) and (38). And the wave dynamics of $u_6^{|3|}$ with condition (42) are shown by Remark 4.3.

Remark 4.1 By setting parameter values of $\beta = 1$, $\alpha = -1$, $p_1 = -1$, $q_1 = \frac{4}{5}$, and $t = 0$ for $u_2^{|1|}$. The 3D and density graphics of first-order breather wave solution are shown in Figs. 2(a) and 2(d).

Remark 4.2 By setting parameter values of $\beta = 1$, $\alpha = -1$, $p_1 = -1$, $q_1 = \frac{4}{5}$, $p_2 = 1$, $q_2 = \frac{3}{5}$, and $t = 0$ for $u_4^{|2|}$. The 3D and density graphics of second-order breather wave solution are shown in Figs. 2(b) and 2(e).

Remark 4.3 By setting parameter values of $\beta = 1$, $\alpha = -1$, $p_1 = -1$, $q_1 = \frac{4}{5}$, $p_2 = 1$, $q_2 = \frac{7}{10}$, $p_3 = -\frac{4}{5}$, $q_3 = \frac{1}{2}$, and $t = 0$ for $u_6^{|3|}$.

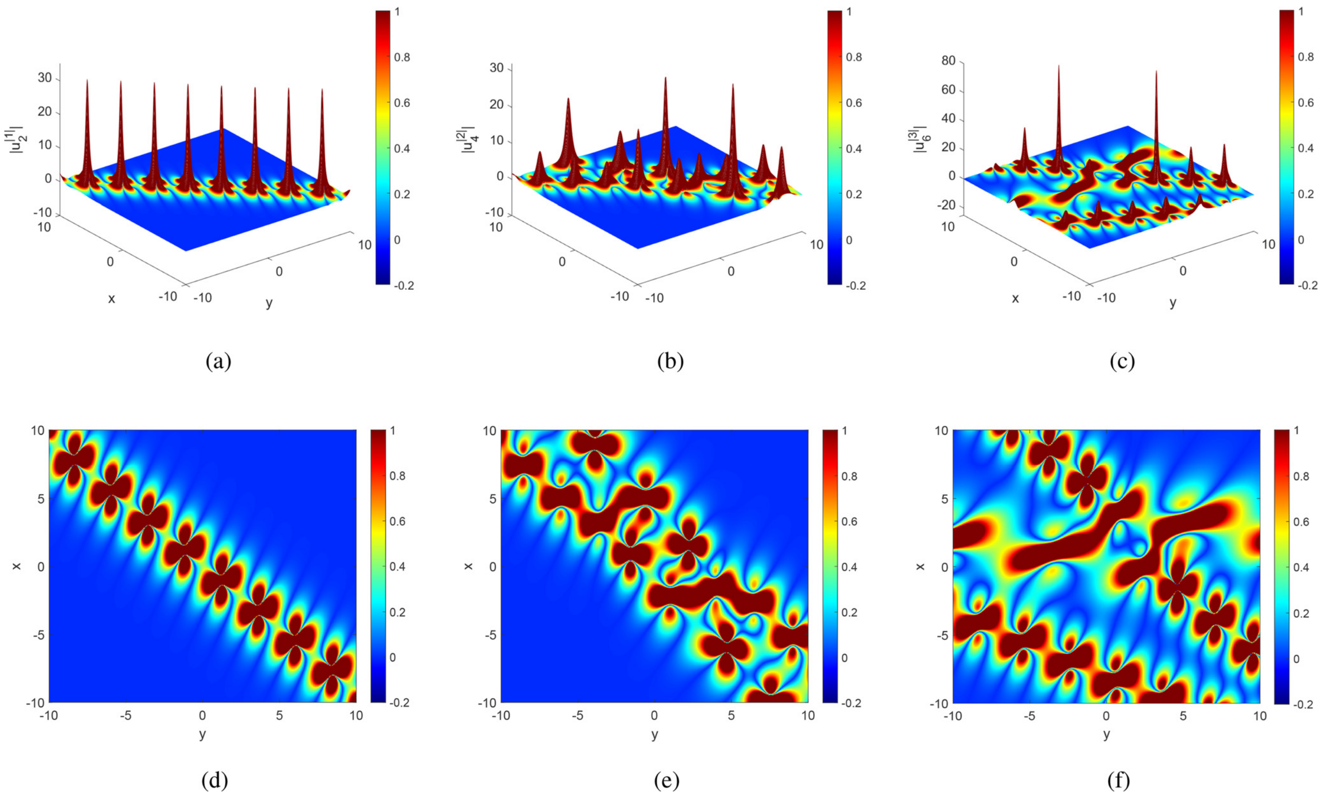

FIG. 2. The 3D (top) and density (bottom) plots of multi-breathers for Eq. (1) generated by the multi-solitons determined by Theorem 1 through conditions (36)–(39). (a) and (d) 1-breather via 2-soliton; (b) and (e) 2-breather via 4-soliton; and (c) and (f) 3-breather via 6-soliton.

The 3D and density graphics of the third-order breather wave solution are shown in Figs. 2(c) and 2(f).

From Fig. 2, it can be observed that there is one breather wave appearing in (a) and (d), two breathers appearing simultaneously in (b) and (e), and three breathers appearing simultaneously in (c) and (f). As we can see, elastic collisions occurred between multi-breathers, and amplitude collapse also occurred near the collision point. This phenomenon is still caused by the influence of nonlinear factors in Eq. (1), but throughout the collision process, like soliton solutions, energy is conserved. The results show that Eq. (1) can give rise to new solutions under specific conditions. In line with this idea, we will continue to give the following new classes of exact traveling wave solutions.

V. MULTI-LUMP WAVES

In this section, we continue to generate another class of interesting multi-wave solutions based on the Hirota condition (12) of N-solitons. In order to obtain the multi-lump wave solutions of Eq. (1), we need to impose additional constraints on condition (12) as follows:

$$\delta_{2m-1}=\delta_{2m}^{*}\triangleq p_m+iq_m,\quad \xi_{2m-1}^{(0)}=\xi_{2m}^{(0)}=i\pi,\quad m=1,2,\ldots, \tag{43}$$

and

$$\begin{cases}\xi_{2m-1}=\xi_{2m}^{*}\triangleq \mathrm{Re.}(\xi_{2m-1})+\mathrm{Im.}(\xi_{2m-1})i=R_m+I_m i,\\ R_m=p_m(x+(3q_m^2-p_m^2)y\\ \quad +\left[(9\beta p_m^2-\alpha)p_m^2+3(\alpha-30\beta p_m^2+15\beta q_m^2)q_m^2\right]t),\\ I_m=q_m(x+(q_m^2-3p_m^2)y\\ \quad +\left[(9\beta q_m^2+\alpha)q_m^2-3(\alpha+30\beta q_m^2-15\beta p_m^2)p_m^2\right]t),\end{cases} \tag{44}$$

now, we make the coefficients $p_m\to 0$ and $q_m\to 0$ before the right side parentheses of R_m and I_m in Eq. (44). And then we can obtain

$$\begin{cases}\hat{\phi}_{2m}=\prod_{i=1}^{2m}\xi_i+\sum_{i<j}\prod_{k\neq i,j}^{2m}\lambda_{ij}\xi_k+\sum_{i<j,\ldots,k<l}^{2m}\underbrace{\lambda_{ij}\cdots\lambda_{kl}}_{M=m},\\ \xi_{2m-1}=\xi_{2m}^{*}\cong\hat{R}_m+\hat{I}_m i,\\ \hat{R}_m=x+(3q_m^2-p_m^2)y\\ \quad +\left[(9\beta p_m^2-\alpha)p_m^2+3(\alpha-30\beta p_m^2+15\beta q_m^2)q_m^2\right]t,\\ \hat{I}_m=x+(q_m^2-3p_m^2)y\\ \quad +\left[(9\beta q_m^2+\alpha)q_m^2-3(\alpha+30\beta q_m^2-15\beta p_m^2)p_m^2\right]t,\end{cases} \tag{45}$$

where $\lambda_{ij}\triangleq\frac{(15\beta p_m^2-5\beta q_m^2+\alpha)q_m^2}{(15\beta q_m^2-5\beta p_m^2-\alpha)p_m^2}>0$. Based on Eq. (11), the multi-lump wave solutions of Eq. (1) can be presented as follows

$$u_{2m}^{|M|}=2\ln(\hat{\phi}_{2m})_{xx},\quad M=m. \tag{46}$$

TABLE I. All cases of "*ij*, *hg*, *kl*" for $\lambda_{ij}\lambda_{hg}\lambda_{kl}$ in Eq. (49).

12,34,56	13,24,56	14,23,56	15,23,46	16,23,45
12,35,46	13,25,46	14,25,36	15,24,36	16,24,35
12,36,45	13,26,45	14,26,35	15,26,34	16,25,34

Case (i). When $M = m = 1$, the first-order lump wave $u_2^{|1|}$ is obtained via Eq. (46), which corresponds to the following condition:

$$\hat{\phi}_2 = \xi_1\xi_2 + \lambda_{12}, \tag{47}$$

where $\xi_i (i = 1, 2)$ satisfy the condition (44) The wave dynamics of $u_2^{|1|}$ with condition (47) will be shown by Remark 5.1.

Case (ii). When $M = m = 2$, the second-order lump wave $u_4^{|2|}$ is presented via Eq. (46), which corresponds to a condition as follows:

$$\hat{\phi}_4 = \xi_1\xi_2\xi_3\xi_4 + \lambda_{12}\xi_3\xi_4 + \lambda_{13}\xi_2\xi_4 + \lambda_{14}\xi_2\xi_3 + \lambda_{23}\xi_1\xi_4 + \lambda_{24}\xi_1\xi_3 + \lambda_{34}\xi_1\xi_2 + \lambda_{12}\lambda_{34} + \lambda_{13}\lambda_{24} + \lambda_{14}\lambda_{23}, \tag{48}$$

where $\xi_i (i = 1, 2, 3, 4)$ also satisfy the condition (44) The wave dynamics of $u_4^{|2|}$ with condition (48) are shown by Remark 5.2.

Case (iii). When $M = m = 3$, the third-order lump wave $u_6^{|3|}$ is presented via Eq. (46), which corresponds to the third condition, namely

$$\hat{\phi}_6 = \prod_{i=1}^{6}\xi_i + \sum_{i<j}\prod_{k\neq i,j}^{6}\lambda_{ij}\xi_k + \sum_{i<j,h<g,k<l}^{6}\lambda_{ij}\lambda_{hg}\lambda_{kl}, \tag{49}$$

where $\xi_i (i = 1, 2, \ldots, 6)$ satisfy the condition (44) The wave dynamics of $u_6^{|3|}$ with condition (49) are shown clearly by Remark 5.3. In addition, all sequence numbers of "*ij*, *hg*, *kl*" in $\lambda_{ij}\lambda_{hg}\lambda_{kl}$ satisfy Table I.

Remark 5.1 By setting the parameter values of $\beta = 1$, $\alpha = -1$, $p_1 = -1$, $q_1 = \frac{4}{5}$, and $t = 0$ for $u_2^{|1|}$ via Eq. (47). The 3D and density graphics of the first-order lump wave are shown in Figs. 3(a) and 3(d).

Remark 5.2 By setting the parameter values of $\beta = 1$, $\alpha = -1$, $p_1 = -1$, $q_1 = \frac{4}{5}$, $p_2 = 1$, $q_2 = \frac{3}{5}$, and $t = 0$ for $u_4^{|2|}$ via Eq. (48). The 3D and density graphics of the second-order lump wave are shown in Figs. 3(b) and 3(e).

Remark 5.3 By setting the parameter values of $\beta = 1$, $\alpha = -1$, $p_1 = -1$, $q_1 = \frac{4}{5}$, $p_2 = 1$, $q_2 = \frac{3}{5}$, $p_3 = -\frac{6}{5}$, $q_3 = 1$, and $t = 0$ for $u_6^{|3|}$ via Eq. (49). The 3D and density graphics of the third-order lump wave are shown in Figs. 3(c) and 3(f).

By observing Fig. 3, we find that when the long-wave limit is taken for multi-solitons, the energy can be highly concentrated. Thereby forming spatially localized solitary waves, which can be used to analyze the generation mechanism and dynamic properties of those rogue waves in the ocean. This characteristic stems from the dynamic balance between nonlinear effects and dispersion in integrable equations.

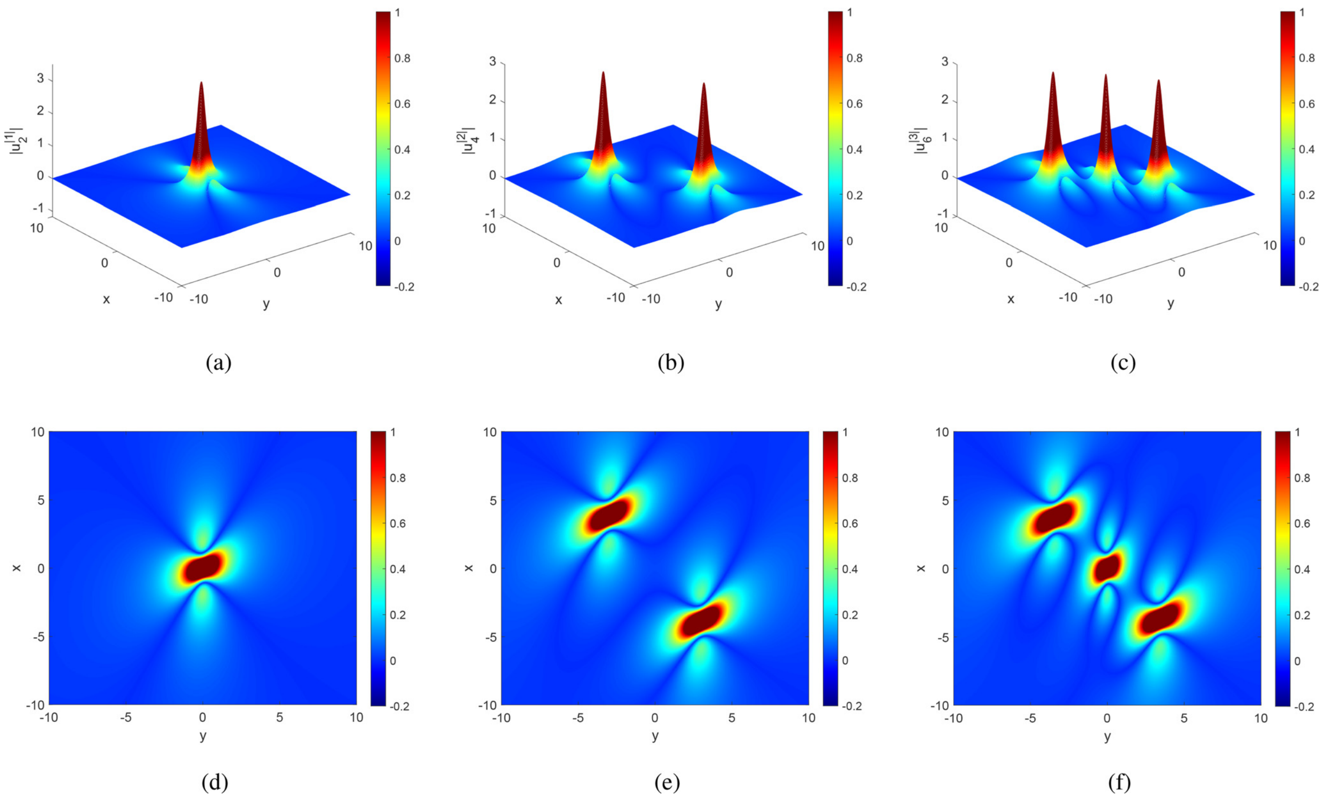

FIG. 3. Through the long-wave limit for condition (12) to present multi-lump solutions for Eq. (1). (a) and (d) first-order lump wave; (b) and (e) second-order lump wave; and (c) and (f) third-order lump wave.

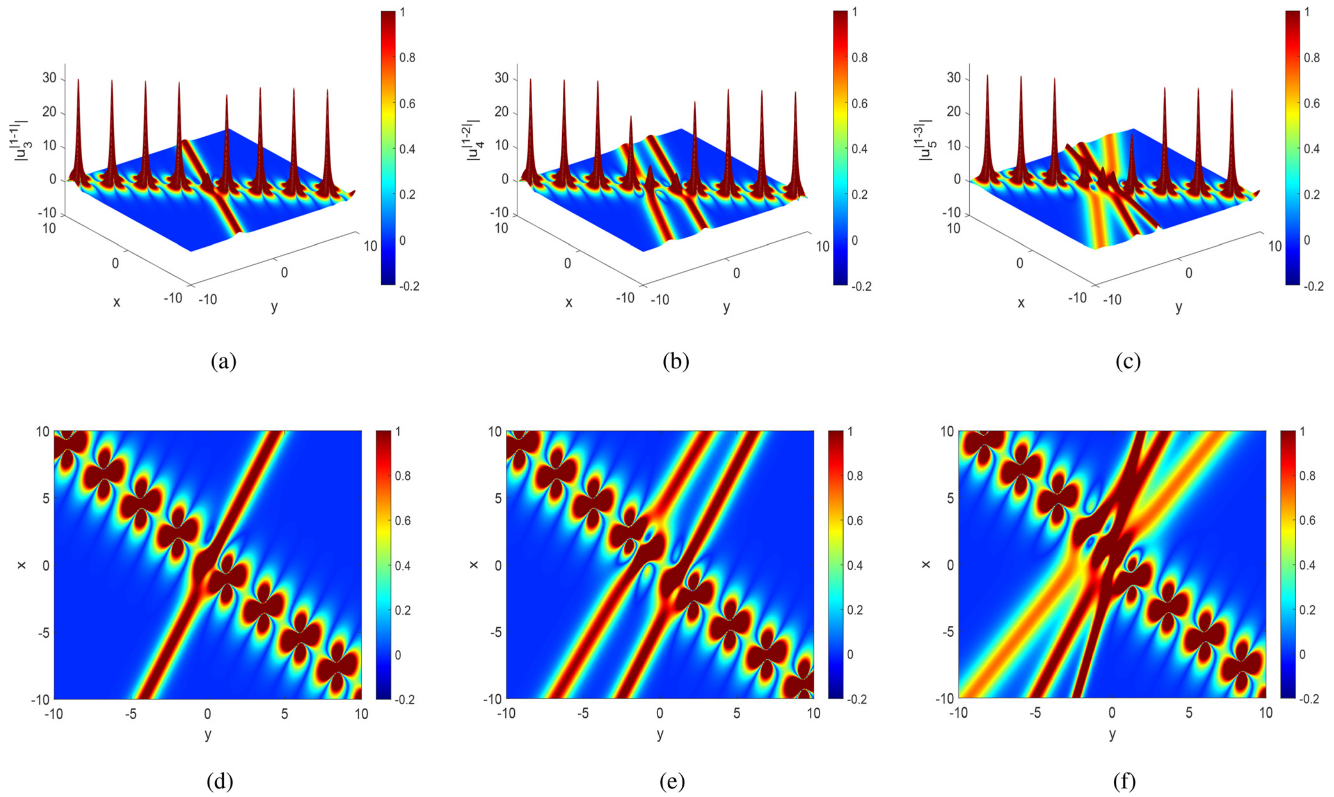

FIG. 4. The interaction phenomena between 1-breather wave and multi-solitons. (a) and (d) 1-breather and 1-soliton; (b) and (e) 1-breather and 2-soliton; and (c) and (f) 1-breather and 3-soliton.

VI. HYBRID WAVES

In the above two sections, two types of multi-wave solutions are provided by applying two special constraints to Eq. (12). In this section, we further impose novel constraints on the Hirota condition (12) to derive the following two types of hybrid multi-wave interaction solutions.

A. Breather-soliton waves

To obtain the first type of hybrid wave solutions between M-breathers and K-solitons of Eq. (1), we need to impose the following constraints on the Hirota condition (12) namely,

$$\begin{cases} \delta_{2m-1} = \delta_{2m}^{*} \triangleq p_m + iq_m,\ \xi_{2m-1}^{(0)} = \xi_{2m}^{(0)} = 0, \quad m = 1, 2, \ldots, \\ \delta_{2m+K} = \delta_{2m+K},\ \xi_{2m+K}^{(0)} = \xi_{2m+K}^{(0)}, \quad K = 1, 2, \ldots, \end{cases} \tag{50}$$

where δ_{2m+K} and $\xi_{2m+K}^{(0)}$ still satisfy Eq. (12), and do not need to be changed. Then Eq. (12) is rewritten in the following form:

$$\begin{cases} \phi_{2m+K} = 1 + \sum_{\rho_i=0,1} \exp\left(\sum_{1\le i<j}^{2m+K} \rho_i\rho_j\theta_{ij} + \sum_{i=1}^{2m+K} \rho_i\xi_i \right), \\ \xi_{2m-1} = \xi_{2m}^{*} \triangleq \mathrm{Re.}(\xi_{2m-1}) + \mathrm{Im.}(\xi_{2m-1})i = R_m + I_m i, \\ \xi_{2m+K} = \xi_{2m+K}\ (\text{Unchanged}), \quad K = 1, 2, \ldots, \end{cases} \tag{51}$$

and

$$\begin{cases} R_m = p_m x + p_m(3q_m^2 - p_m^2)y \\ \qquad + p_m\left[(9\beta p_m^2 - \alpha)p_m^2 + 3(\alpha - 30\beta p_m^2 + 15\beta q_m^2)q_m^2\right]t, \\ I_m = q_m x + q_m(q_m^2 - 3p_m^2)y \\ \qquad + q_m\left[(9\beta q_m^2 + \alpha)q_m^2 - 3(\alpha + 30\beta q_m^2 - 15\beta p_m^2)p_m^2\right]t, \end{cases} \tag{52}$$

where $\lambda_{ij} \triangleq \mathrm{e}^{\theta_{ij}}$ is given in Eq. (38). Substituting Eqs. (51) and (52) back into Eq. (11), the hybrid breather-soliton solutions of Eq. (1) can be presented as follows:

$$u_{2m+K}^{|M-K|} = 2\ln(\phi_{2m+K})_{xx}, \quad M = m. \tag{53}$$

Figures 4 and 5 reveal the interaction phenomena between multi-breathers and multi-solitons. It is not difficult to see that elastic collisions occur between mixed-type multiple waves. At the collision point with the solitons, there is a significant amplitude collapse phenomenon of the breather wave, accompanied by a slight phase shift, but the direction of wave propagation remains unchanged. This indicates that the breather waves excited by the integrable equation under specific conditions are still elastic with solitons. The new hybrid breather-soliton waves retain the property of energy conservation of the original equation. These interaction phenomena help to reveal the evolutionary behavior after collisions between different types of shallow-water waves in the ocean.

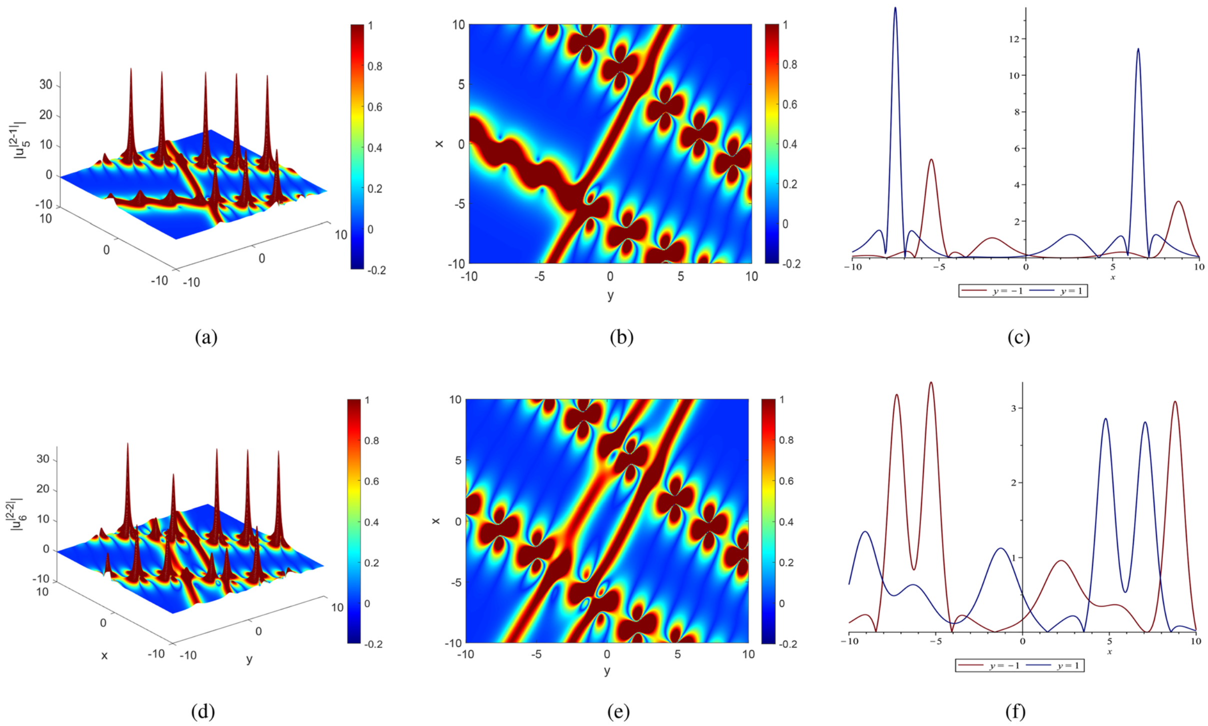

FIG. 5. The interaction phenomena between 2-breather wave and multi-solitons. (a)–(c) 2-breather and 1-soliton; and (d)–(f) 2-breather and 2-soliton.

Remark 6.1.1 When $M = m = 1$ and $K = 1$, the 1-breather and 1-soliton mixed-type wave $u_3^{|1-1|}$ is obtained via Eq. (53). By setting parameter values of $\beta = 1,\ \alpha = -1,\ p_1 = -1,\ q_1 = \frac{4}{5},\ \delta_3 = \frac{3}{2}$, $\xi_3^{(0)} = 0$, and $t = 0$, the 3D and density plots of $u_3^{|1-1|}$ are shown in Figs. 4(a) and 4(d).

Remark 6.1.2 When $M = m = 1$ and $K = 2$, the 1-breather and 2-soliton mixed-type wave $u_4^{|1-2|}$ is presented via Eq. (53). By setting parameter values of $\beta = 1,\ \alpha = -1,\ p_1 = -1,\ q_1 = \frac{4}{5},\ \delta_3 = -\frac{7}{5}$, $\delta_4 = \frac{3}{2}$, $\xi_3^{(0)} = \xi_4^{(0)} = 0$, and $t = 0$, the 3D and density plots of $u_4^{|1-2|}$ are shown in Figs. 4(b) and 4(e).

Remark 6.1.3 When $M = m = 1$ and $K = 3$, the 1-breather and 3-soliton mixed-type wave $u_5^{|1-3|}$ is presented via Eq. (53). By setting parameter values of $\beta = 1$, $\alpha = -1$, $p_1 = -1$, $q_1 = \frac{4}{5}$, $\delta_3 = 2$, $\delta_4 = \frac{6}{5}$, $\delta_5 = \frac{3}{2}$, $\xi_i^{(0)}(i = 3, 4, 5) = 0$, and $t = 0$, the 3D and density plots of $u_5^{|1-3|}$ are shown in Figs. 4(c) and 4(f).

Remark 6.1.4 When $M = m = 2$ and $K = 1$, the 2-breather and 1-soliton mixed-type wave $u_5^{|2-1|}$ is presented via Eq. (53). By setting parameter values of $\beta = 1$, $\alpha = -1$, $p_1 = -1$, $q_1 = \frac{4}{5}$, $p_2 = 1$, $q_2 = \frac{3}{4}$, $\delta_5 = \frac{3}{2}$, $\xi_5^{(0)} = 0$ and $t = 0$, the 3D and 2D plots of $u_5^{|2-1|}$ are shown in Figs. 5(a)–5(c).

Remark 6.1.5 When $M = m = 2$ and $K = 2$, the 2-breather and 2-soliton mixed-type wave $u_6^{|2-2|}$ is presented via Eq. (53). By setting parameter values of $\beta = 1$, $\alpha = -1$, $p_1 = -1$, $q_1 = \frac{4}{5}$, $p_2 = 1$, $q_2 = \frac{3}{4}$, $\delta_5 = -\frac{7}{5}$, $\delta_6 = \frac{3}{2}$, $\xi_5^{(0)} = \xi_6^{(0)} = 0$, and $t = 0$, the 3D and 2D plots of $u_6^{|2-2|}$ are shown in Figs. 5(d)–5(f).

B. Lump-soliton waves

When the long-wave limit of the N-solitons of an integrable equation is taken, the energy of every two adjacent solitons will be concentrated within a certain local range in space, thus forming lump waves or rogue waves.[15,37,38] In order to obtain another type of hybrid wave solutions between M-lumps and K-solitons of Eq. (1), we also need to impose some constraints on condition (12) as follows:

$$\begin{cases} \delta_{2m-1} = \delta_{2m}^{*} \triangleq p_m + iq_m,\ \xi_{2m-1}^{(0)} = \xi_{2m}^{(0)} = i\pi, \quad m = 1, 2, \ldots, \\ \delta_{2m+K} = \delta_{2m+K},\ \xi_{2m+K}^{(0)} = \xi_{2m+K}^{(0)}, \quad K = 1, 2, \ldots, \end{cases} \tag{54}$$

where δ_{2m+K} and $\xi_{2m+K}^{(0)}$ also satisfy Eq. (12) and are not to be changed. Then Eq. (12) can be rewritten as a new form based on Eq. (45), that is,

$$\begin{cases} \hat{\phi}_{2m+K} = \prod_{i=1}^{2m} \xi_i + \sum_{i<j} \prod_{k\neq i,j}^{2m} \lambda_{ij}\xi_k + \sum_{i<j,\ldots,k<l}^{2m} \underbrace{\lambda_{ij}\cdots\lambda_{kl}}_{M=m} \\ \qquad + \sum_{\rho_i=0,1} \exp\left(\sum_{1\le i<j}^{2m+K} \rho_i\rho_j\theta_{ij} + \sum_{i=2m+1}^{2m+K} \rho_i\xi_i \right), \\ \xi_{2m-1} = \xi_{2m}^{*} \triangleq \mathrm{Re.}(\xi_{2m-1}) + \mathrm{Im.}(\xi_{2m-1})i = \hat{R}_m + \hat{I}_m i, \\ \xi_{2m+K} = \xi_{2m+K}\ (\text{Unchanged}), \quad K = 1, 2, \ldots, \end{cases} \tag{55}$$

and

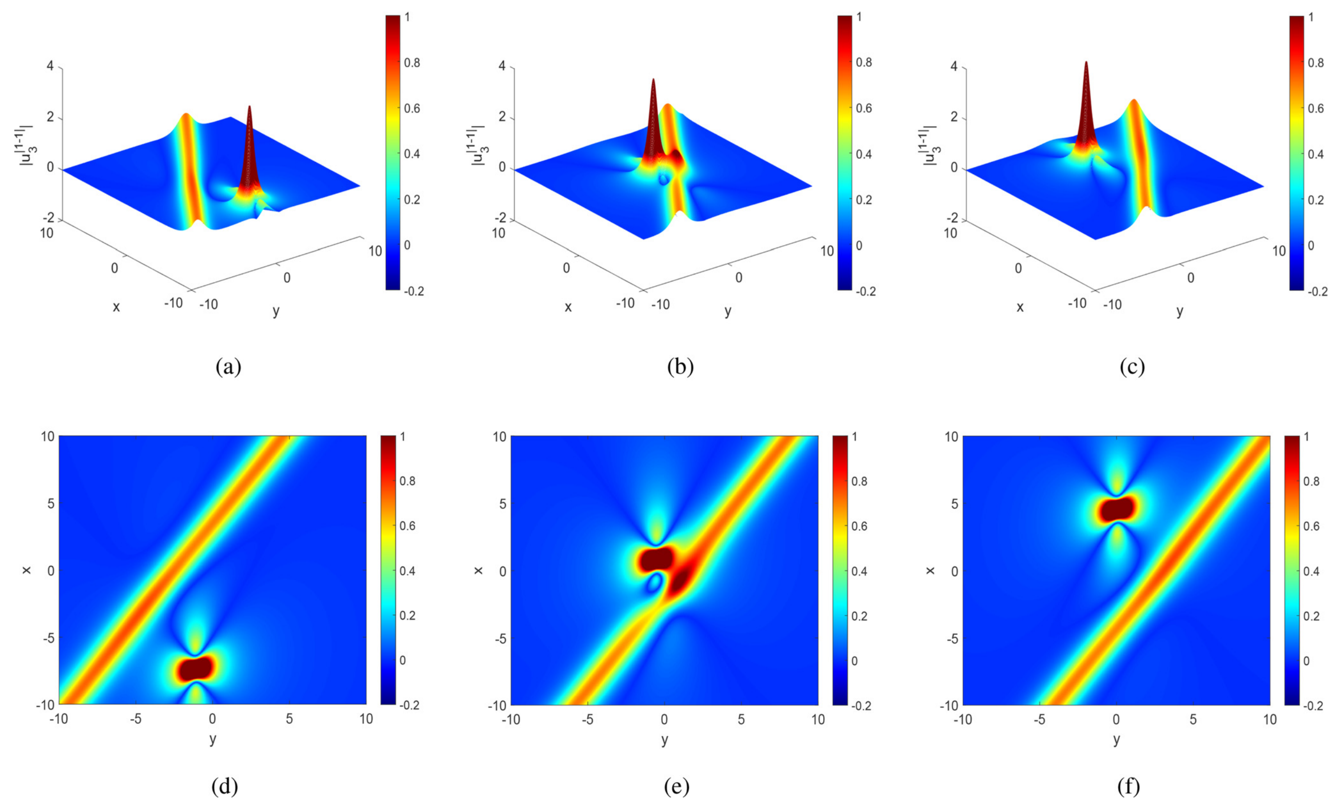

FIG. 6. The evolution phenomena of elastic collision between 1-lump and 1-soliton. (a) and (d) $t=-\frac{1}{4}$; (b) and (e) $t=0$; and (c) and (f) $t=\frac{1}{8}$.

$$\begin{cases} \hat{R}_m = x + (3q_m^2 - p_m^2)y \\ \qquad +\left[(9\beta p_m^2 - \alpha)p_m^2 + 3(\alpha - 30\beta p_m^2 + 15\beta q_m^2)q_m^2\right]t, \\ \hat{I}_m = x + (q_m^2 - 3p_m^2)y \\ \qquad +\left[(9\beta q_m^2 + \alpha)q_m^2 - 3(\alpha + 30\beta q_m^2 - 15\beta p_m^2)p_m^2\right]t, \end{cases} \tag{56}$$

where $\lambda_{ij} \triangleq e^{\theta_{ij}}$ still satisfies Eq. (38). Substituting Eqs. (55) and (56) back into Eq. (11), the hybrid lump-soliton solutions of Eq. (1) are presented, namely

$$u_{2m+K}^{|M-K|} = 2\ln(\hat{\phi}_{2m+K})_{xx}, \quad M = m. \tag{57}$$

Figures 6–8 show the entire process of the interaction between multi-lumps and multi-solitons. We can easily see that as the lump wave approaches the stripe solitons and collides, the stripe solitons will collapse, and the lump wave will completely pass through the other side of the solitons. From (b) and (e) in Fig. 7, it can be seen that there was a brief energy exchange at the collision point. These phenomena indicate that the lump waves excited by the integrable equation under Hirota N-solitons condition are still elastic with solitons. The new hybrid lump-soliton waves conform to the dynamic balance between linear dispersion and nonlinear disturbance in Eq. (1).

Remark 6.2.1 When $M=m=1$ and $K=1$, the 1-lump and 1-soliton mixed-type wave $u_3^{|1-1|}$ is presented via Eq. (57). By setting parameter values of $\beta=1$, $\alpha=-1$, $p_1=-1$, $q_1=\frac{9}{10}$, $\delta_3=\frac{6}{5}$, $\xi_3^{(0)}=2$, and t from $-\frac{1}{4}$ to $\frac{1}{8}$, the 3D and 2D evolution plots of $u_3^{|1-1|}$ are shown in Fig. 6.

Remark 6.2.2 When $M=m=1$ and $K=2$, the 1-lump and 2-soliton mixed-type wave $u_4^{|1-2|}$ is obtained via Eq. (57). By setting parameter values of $\beta=1$, $\alpha=-1$, $p_1=-1$, $q_1=\frac{4}{5}$, $\delta_3=\frac{6}{5}$, $\delta_4=1$, $\xi_3^{(0)}=\frac{3}{2}$, $\xi_4^{(0)}=\frac{7}{5}$, and t from $-\frac{1}{5}$ to $\frac{1}{5}$, the 3D and 2D evolution plots of $u_4^{|1-2|}$ are shown in Fig. 7.

Remark 6.2.3 When $M=m=2$ and $K=1$, the 2-lump and 1-soliton mixed-type wave $u_5^{|2-1|}$ is presented via Eq. (57). By setting parameter values of $\beta=1$, $\alpha=-1$, $p_1=1$, $q_1=\frac{4}{5}$, $p_2=-1$, $q_2=\frac{3}{5}$, $\delta_5=1$, $\xi_5^{(0)}=1$, and t from $-\frac{1}{5}$ to $\frac{1}{8}$, the 3D and 2D evolution plots of $u_5^{|2-1|}$ are shown in Fig. 8.

VII. MESHY-PERIODIC LUMP WAVES

In this section, the BNNM[40] is used to construct a novel class of multi-periodic lump waves for Eq. (1), known as meshy-periodic lump wave solutions. Based on Eq. (13), we assume that the function ϕ in $B_{mKP}(\phi)$ Eq. (9) has a multi-layer network structure (see Fig. 9). The output layer in Fig. 9 covers two hidden layers. When the two neurons in the first hidden layer are set to $\sigma_1=\sin(\xi_1)$ and $\sigma_2=\cos(\xi_2)$, and the three neurons in the second hidden layer are set to $\sigma_3=-(\delta_{1,3}\sigma_1 + \delta_{2,3}\sigma_2 + \xi_2^{(3)})$, $\sigma_4=(\delta_{1,4}\sigma_1+\delta_{2,4}\sigma_2+\xi_2^{(4)})^2$, and $\sigma_5=(\delta_{1,5}\sigma_1 + \delta_{2,5}\sigma_2+\xi_2^{(5)})^2$, we have

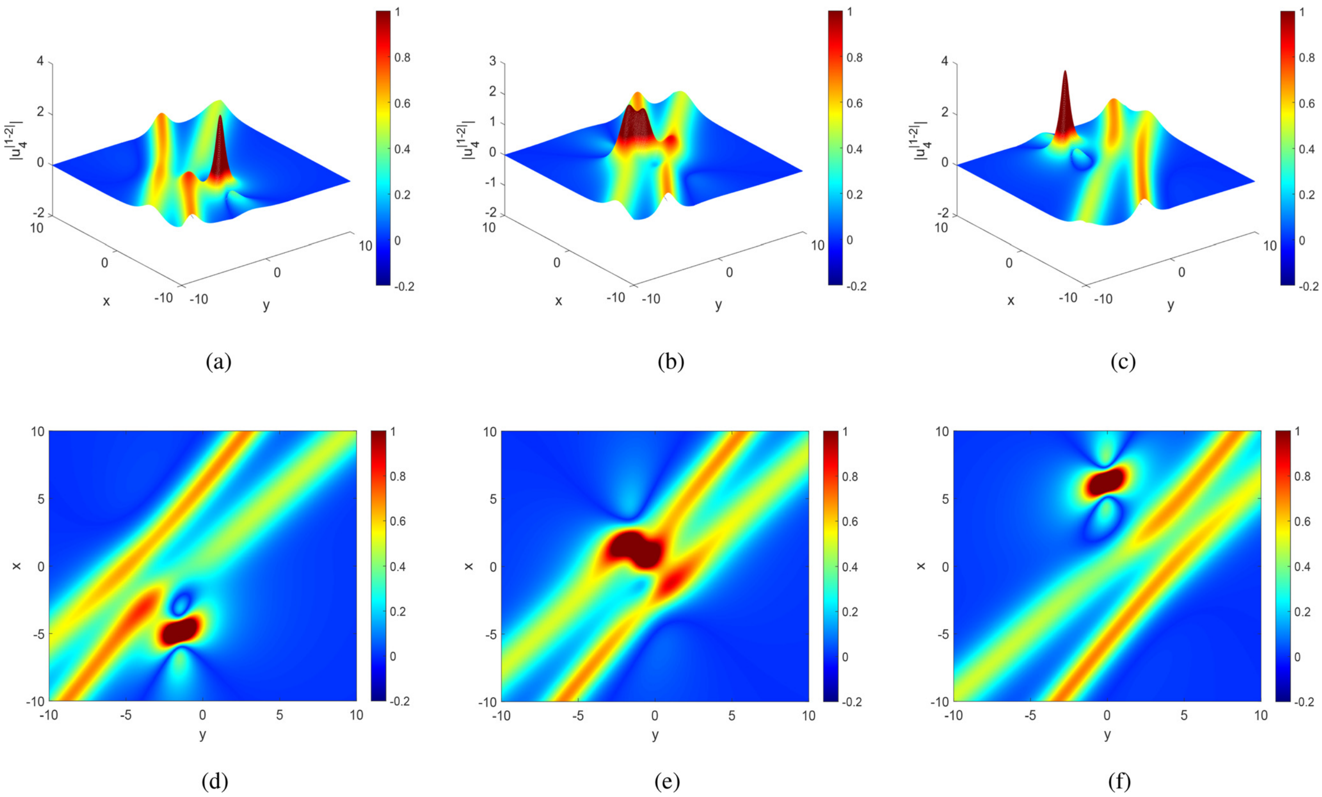

FIG. 7. The evolution phenomena of elastic collision between 1-lump and 2-soliton. (a) and (d) $t=-\frac{1}{5}$; (b) and (e) $t=0$; and (c) and (f) $t=\frac{1}{5}$.

$$\begin{cases} \phi = 1+\sin(\xi_1)+\cos(\xi_2)-\xi_3+\xi_4^2+\xi_5^2, \\ \xi_j = \delta_{1,j}\sin(\xi_1)+\delta_{2,j}\cos(\xi_2)+\xi_2^{(j)}, \quad j=3,4,5, \\ \xi_i = \delta_{x,i}x+\delta_{y,i}y+\delta_{t,i}t+\xi_1^{(i)}, \quad i=1,2, \end{cases} \tag{58}$$

where $\delta_{\hat{k},\hat{l}}(\langle\hat{k}=x,y,t,1,2\rangle,\langle\hat{l}=1,2,3,4,5\rangle,\hat{k}\neq\hat{l})$, $\xi_1^{(i)}(i=1,2)$, and $\xi_2^{(j)}(j=3,4,5)$ are undetermined real constants. Substituting expression (58) into Eq. (9) to obtain a polynomial consisting of ϕ and its partial derivatives. By setting the sum of the same power coefficients of ϕ and $\partial\phi$ to zero, a system of nonlinear algebraic equations can be obtained. Solving this nonlinear algebraic system, we get

$$\begin{gathered} \alpha = 20\beta\delta_{x,2}^2, \quad \beta=\beta, \quad \gamma=0, \quad \delta_{1,3}=\delta_{1,3}, \\ \delta_{1,4} = -\frac{\delta_{1,5}\delta_{2,5}}{\delta_{2,4}}, \quad \delta_{1,5}=\delta_{1,5}, \\ \delta_{2,3} = 2\delta_{2,4}\xi_2^{(4)}+2\delta_{2,5}\xi_2^{(5)}+1, \quad \delta_{2,4}=\delta_{2,4}, \quad \delta_{2,5}=\delta_{2,5}, \\ \delta_{t,1}=0, \quad \delta_{t,1}=64\beta\delta_{x,2}^5, \\ \delta_{x,1}=0, \quad \delta_{x,2}=\delta_{x,2}, \quad \delta_{y,i}=\delta_{y,i}(i=1,2), \\ \xi_1^{(i)}=\xi_1^{(i)}(i=1,2), \quad \xi_2^{(j)}=\xi_2^{(j)}(j=3,4,5), \end{gathered} \tag{59}$$

substituting Eq. (59) back into Eq. (58) and using the direct relation (13) a meshy-periodic lump wave solution is presented below

$$\begin{aligned} u = \frac{4}{\phi^2}(&2\cos(\xi_2)^4\delta_{2,5}^4+4(\sin(\xi_1)\delta_{1,5}\delta_{2,5} \\ &-\delta_{2,4}(\xi_2^{(4)}-\xi_4))\delta_{2,5}^2\cos(\xi_2)^3-(4\delta_{1,5}\delta_{2,4}\delta_{2,5}(\xi_2^{(4)}-\xi_4)\sin(\xi_1) \\ &+2\cos(\xi_1)^2\delta_{1,5}^2\delta_{2,5}^2+2\delta_{2,5}^4+(2\phi-2\delta_{1,5}^2)\delta_{2,5}^2 \\ &+\delta_{2,4}^2(-2\xi_2^{(4)2}+4\xi_2^{(4)}\xi_4-2\xi_4^2+\phi))\cos(\xi_2)^2 \\ &-(\sin(\xi_1)\delta_{1,5}\delta_{2,5}-\delta_{2,4}(\xi_2^{(4)}-\xi_4))(4\delta_{2,5}^2+\phi)\cos(\xi_2) \\ &+4\delta_{1,5}\delta_{2,4}\delta_{2,5}(\xi_2^{(4)}-\xi_4)\sin(\xi_1)+2\cos(\xi_1)^2\delta_{1,5}^2\delta_{2,5}^2 \\ &-(2\delta_{1,5}^2-\phi)\delta_{2,5}^2+\delta_{2,4}^2(-2\xi_2^{(4)2}+4\xi_2^{(4)}\xi_4-2\xi_4^2+\phi))\delta_{x,2}^2. \end{aligned} \tag{60}$$

Figure 10 shows the wave dynamics of the meshy-periodic lump wave solution (60) with some 3D and 2D plots. It is not difficult to see from the figures that we obtain a new kind of exact traveling wave solution for Eq. (1), through a test function ϕ with multi-layer network structure. This result can be used to describe shallow-water waves with a network structure that often occur near the coastline. In addition, the neural network structure utilizing test functions has potential application value in revealing turbulence phenomena.

Remark 7.1 By assigning the values of $\beta=1$, $\delta_{1,3}=-0.01$, $\delta_{1,5}=1$, $\delta_{2,4}=1$, $\delta_{2,5}=0.02$, $\delta_{x,2}=0.2$, $\delta_{y,1}=-0.5$, $\delta_{y,2}=0.05$, $\xi_1^{(i)}(i=1,2)=\xi_2^{(j)}(j=3,4,5)=1$, and $t=0$ for dynamic plots of meshy-periodic lump wave solution (60).

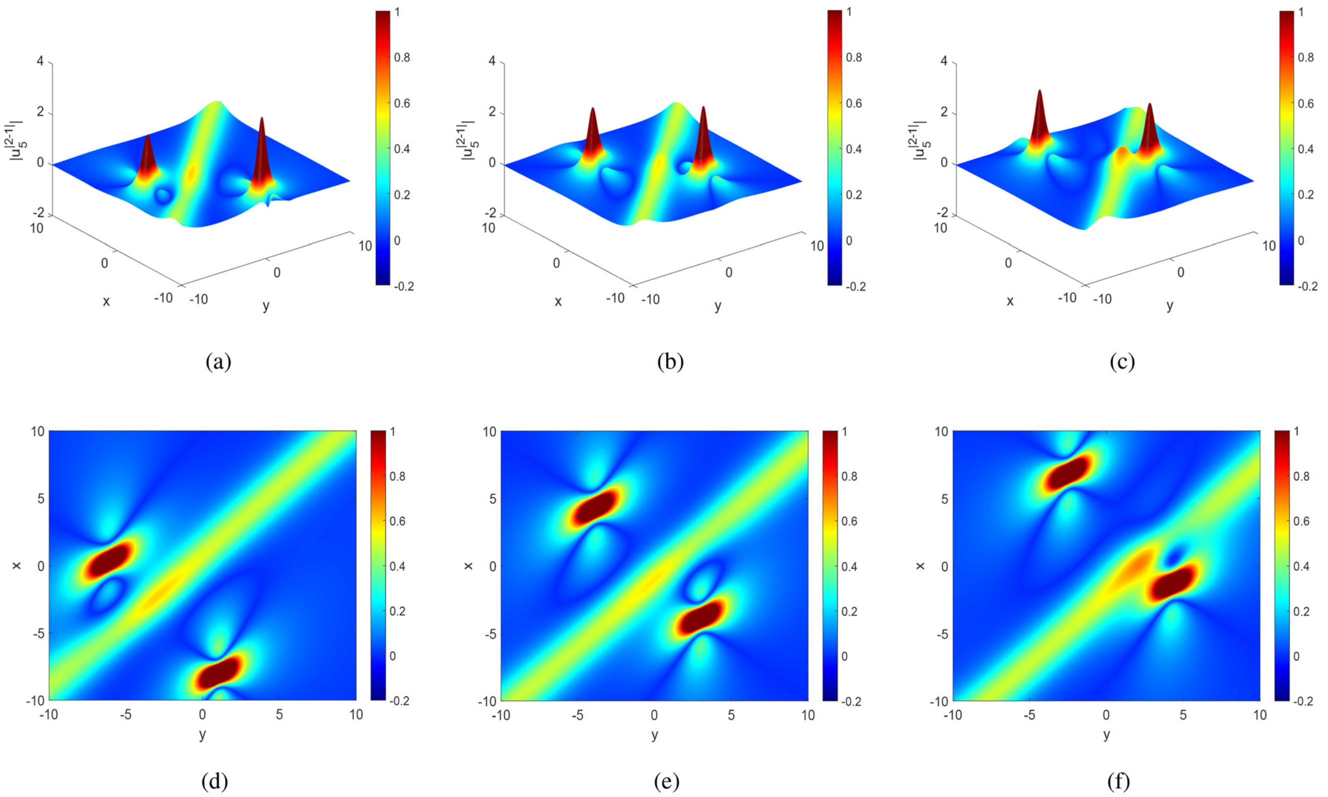

FIG. 8. The evolution phenomena of elastic collision between 2-lump and 1-soliton. (a) and (d $t=-\frac{1}{5}$; (b) and (e) $t=0$; and (c) and (f) $t=\frac{1}{8}$.

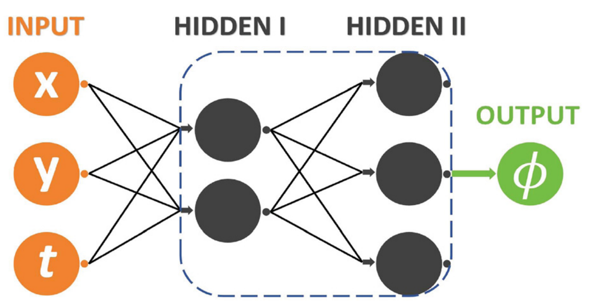

FIG. 9. The multi-layer neural network structure of the tensor function ϕ in BNNM.

VIII. CONCLUSIONS

In this article, we obtained rich multi-wave solutions of the shallow-water wave Eq. (1) and studied various nonlinear elastic collision phenomena. Through a second-order logarithmic derivative transformation, the bilinear form of Eq. (1) under the coefficient condition of integrability was given. Based on $\mathrm{HB}_{\mathrm{mKP}}(\phi)$ Eq. (10), the Hirota standard condition of N-soliton solutions for Eq. (1) was presented. The soliton dynamics of N-soliton solutions were clearly shown (see Fig. 1). The geometric and dynamic characteristics of solitons were completely revealed.

In particular, we obtained multi-breather waves (see Fig. 2), multi-lump waves (see Fig. 3), and several types of hybrid multi-wave solutions (see Figs. 4–8) by applying specific constraints to the coefficient conditions of N-solitons. The 3D and 2D graphs of these results shown that the nonlinear waves with elastic structures, and the amplitude decreases at the site of collision. The interaction phenomena of these nonlinear multi-waves can well describe the fusion and fission behavior of solitons. It is worth mentioning that, based on the mixed-type breather-soliton waves given in Sec. VI A, we can still take the long-wave limit for multi-solitons in Eqs. (50)–(52), that is,

$$\begin{cases} \delta_{2m-1}=\delta_{2m}^{*}\triangleq p_m+iq_m,\ \xi_{2m-1}^{(0)}=\xi_{2m}^{(0)}=0, \\ \delta_{2m+1}=\delta_{2m+2}^{*}\triangleq p_m+iq_m,\ \xi_{2m+1}^{(0)}=\xi_{2m+2}^{(0)}=i\pi, \\ \xi_{2m-1}=\xi_{2m}^{*}\triangleq \mathrm{Re.}(\xi_{2m-1})+\mathrm{Im.}(\xi_{2m-1})i=R_m+I_m i, \\ \xi_{2m+1}=\xi_{2m+2}^{*}\triangleq \mathrm{Re.}(\xi_{2m+1})+\mathrm{Im.}(\xi_{2m+1})i=\hat{R}_m+\hat{I}_m i, \end{cases} \tag{61}$$

and

$$\begin{cases} R_m=p_m x+p_m(3q_m^2-p_m^2)y \\ \qquad +p_m\left[(9\beta p_m^2-\alpha)p_m^2+3(\alpha-30\beta p_m^2+15\beta q_m^2)q_m^2\right]t, \\ I_m=q_m x+q_m(q_m^2-3p_m^2)y \\ \qquad +q_m\left[(9\beta q_m^2+\alpha)q_m^2-3(\alpha+30\beta q_m^2-15\beta p_m^2)p_m^2\right]t, \\ \hat{R}_m=x+(3q_m^2-p_m^2)y \\ \qquad +\left[(9\beta p_m^2-\alpha)p_m^2+3(\alpha-30\beta p_m^2+15\beta q_m^2)q_m^2\right]t, \\ \hat{I}_m=x+(q_m^2-3p_m^2)y \\ \qquad +\left[(9\beta q_m^2+\alpha)q_m^2-3(\alpha+30\beta q_m^2-15\beta p_m^2)p_m^2\right]t. \end{cases} \tag{62}$$

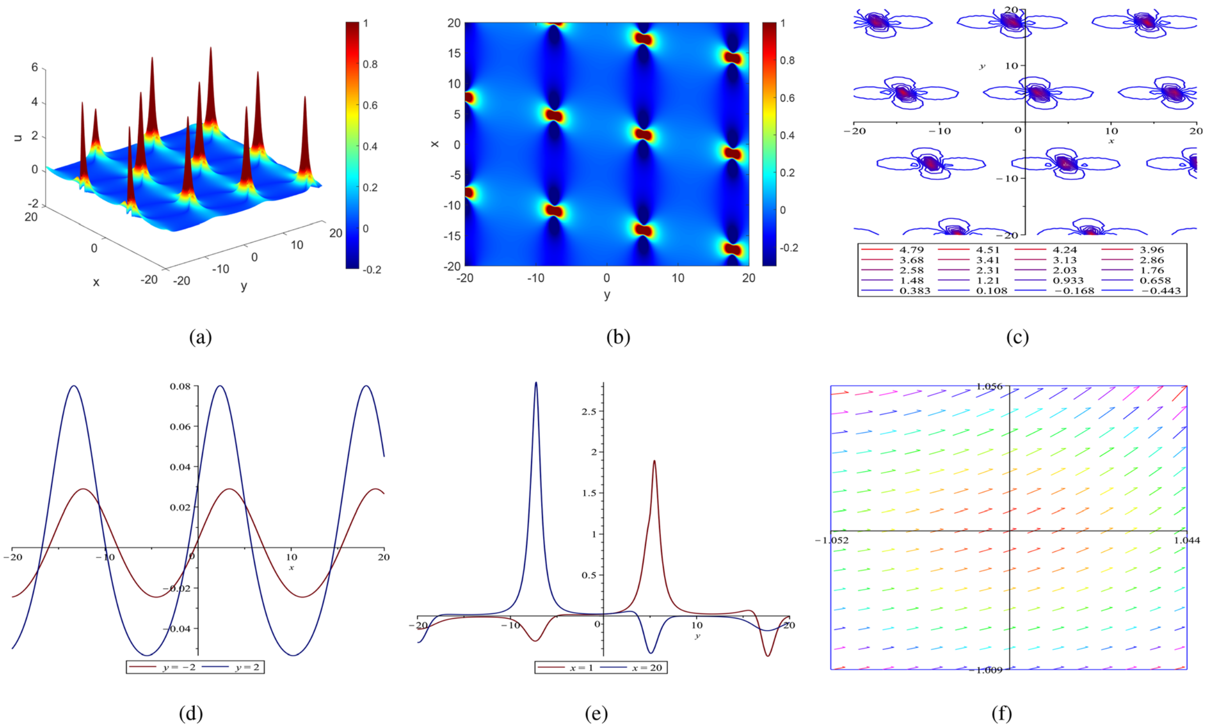

FIG. 10. Profiles of meshy-periodic lump wave solution (60). (a) 3D plot; (b) Density plot; (c) Contour plot; (d) x-curves; (e) y-curves; and (f) $\mathbf{grad}\, u$ at $(x, y) \in [-1, 1] \times [-1, 1]$.

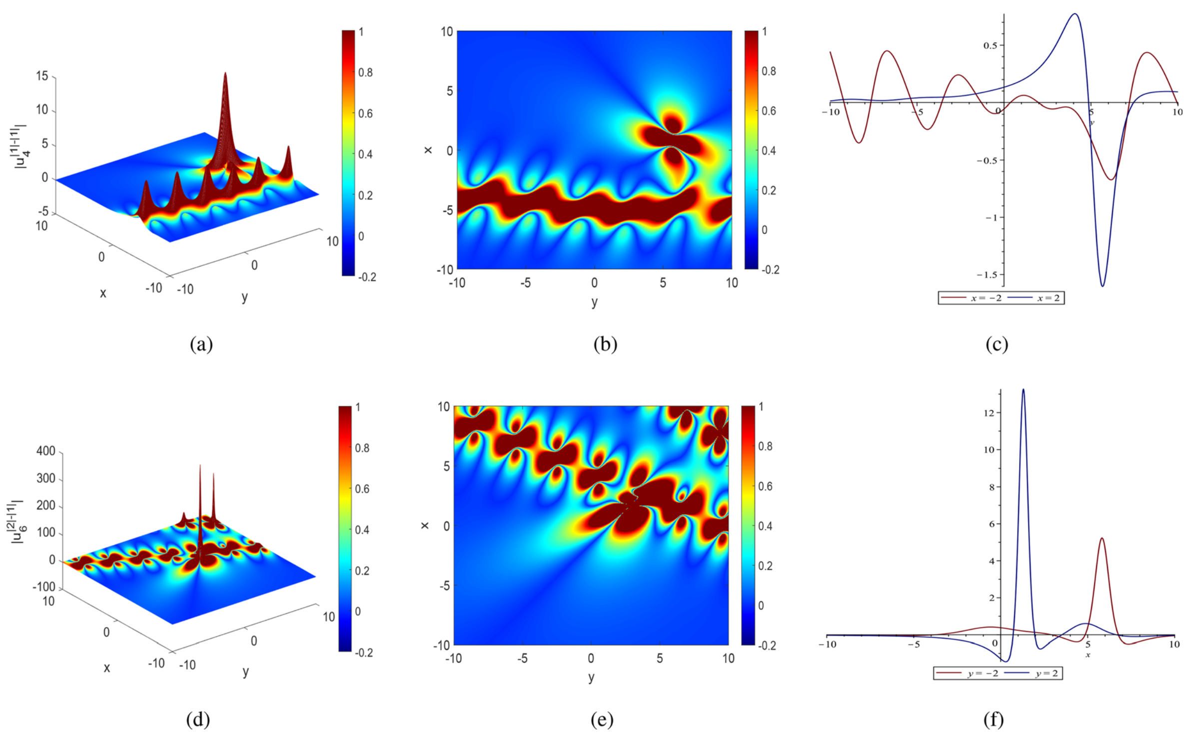

FIG. 11. Profiles of breather-lump wave solutions $u_4^{|1|-|1|}$ (top) and $u_6^{|2|-|1|}$ (bottom). (a) and (d) 3D plots; (b) and (e) density plots; (c) y-curves; and (f) x-curves.

By utilizing the two new conditions provided by Eqs. (61) and (62) and further combining them with Eq. (53), we can obtain a new class of hybrid multi-wave solutions, namely breather-lump waves. The two cases of $m = 1$ and $m = 2$ are shown in Fig. 11, with the values of $\alpha = -1$, $\beta = 1$, $p_1 = -\frac{3}{5}$, $q_1 = \frac{4}{5}$, $p_2 = 1$, $q_2 = \frac{3}{5}$, and $t = -\frac{1}{5}$ for (a)–(c); and the values of $\alpha = -1$, $\beta = 1$, $p_1 = \frac{4}{5}$, $q_1 = -\frac{2}{5}$, $p_2 = -1$, $q_2 = \frac{4}{5}$, $p_3 = 1$, $q_3 = -\frac{7}{10}$, and $t = \frac{3}{10}$ for (d)–(f). The above four types of derived wave solutions well reveal the interaction phenomena of shallow-water waves after they collide with each other. It also reflects that Eq. (1) can generate both local and nonlocal waves.

In addition, we obtained a type of meshy-periodic lump waves of Eq. (1) via a new objective function based on a neural network model with multi-layer structure. The plots of this solution showed a class of multi-periodic lump waves (see Fig. 10). Furthermore, it will be very interesting to construct various exact traveling wave solutions of Eq. (1), by using more test functions.[19,34–41] In particular, the integrability condition $\alpha_1 = 6\alpha$ and $\beta_2 = 3\beta_1 = 45\beta$ of Eq. (1) is crucial for obtaining bilinear form, N-soliton solutions and several other derived wave solutions. The Painlevé analysis[37,38] for Eq. (1) is another key focus of our work, which will not be emphasized in this article. In our future work, we will also focus on the Darboux transformation[15,16] for Eq. (1).

ACKNOWLEDGMENTS

This research was supported by the Zhejiang Provincial Natural Science Foundation of China under Grant No. LQ24A010017, the National Natural Science Foundation of China under Grant Nos. 12271488, 11975145, and 11972291, and the Ministry of Science and Technology of China (G2021016032L and G2023016011L).

AUTHOR DECLARATIONS

Conflict of Interest

The authors have no conflicts to disclose.

Author Contributions

Litao Gai: Formal analysis (lead); Funding acquisition (equal); Methodology (lead); Project administration (equal); Resources (equal); Software (lead); Writing – original draft (lead). **Wen-Xiu Ma:** Conceptualization (equal); Methodology (equal); Project administration (lead); Supervision (equal); Writing – review & editing (equal). **Lianbao Jin:** Software (equal); Supervision (equal); Validation (equal); Visualization (equal); Writing – review & editing (equal).

DATA AVAILABILITY

Data sharing is not applicable to this article as no new data were created or analyzed in this study.

REFERENCES

[1] L. Khaykovich, F. Schreck, G. Ferrari *et al.*, "Formation of a matter-wave bright soliton," Science **296**, 1290–1293 (2002).
[2] J. Zeng and B. A. Malomed, "Localized dark solitons and vortices in defocusing media with spatially inhomogeneous nonlinearity," Phys. Rev. E **95**, 052214 (2017).
[3] F. Zhao, X. Xu, H. He *et al.*, "Vortex solitons in quasi-phase-matched photonic crystals," Phys. Rev. Lett. **130**, 157203 (2023).
[4] M. Bertola, T. Grava, and G. Orsatti, "Soliton shielding of the focusing nonlinear Schrödinger equation," Phys. Rev. Lett. **130**, 127201 (2023).
[5] H. X. Wu, Y. B. Zeng, and T. Y. Fan, "Soliton, positon and negaton solutions of extended KdV equation," Commun. Theor. Phys. **49**, 529–534 (2008).
[6] J. Q. Mo, "Generalized variational iteration solution of soliton for disturbed KdV equation," Commun. Theor. Phys. **53**, 440–442 (2010).
[7] A. M. Wazwaz, "Soliton solutions of the KdV equation with higher-order corrections," Phys. Scr. **82**, 045005 (2010).
[8] A. M. Wazwaz, "Multiple-soliton solutions of the perturbed KdV equation," Commun. Nonlinear Sci. Numer. Simul. **15**, 3270–3273 (2010).
[9] Z. L. Zhao and L. C. He, "Space-curved resonant solitons and inelastic interaction solutions of a $(2+1)$-dimensional generalized KdV equation," Nonlinear Dyn. **112**, 3823–3833 (2024).
[10] G. Z. Wu and C. Q. Dai, "Nonautonomous soliton solutions of variable-coefficient fractional nonlinear Schrödinger equation," Appl. Math. Lett. **106**, 106365 (2020).
[11] H. B. Han, H. J. Li, and C. Q. Dai, "Wick-type stochastic multi-soliton and soliton molecule solutions in the framework of nonlinear Schrödinger equation," Appl. Math. Lett. **120**, 107302 (2021).
[12] S. S. Shen, Z. J. Yang, Z. G. Pang *et al.*, "The complex-valued astigmatic cosine-Gaussian soliton solution of the nonlocal nonlinear Schrödinger equation and its transmission characteristics," Appl. Math. Lett. **125**, 107755 (2022).
[13] S. Ur Rehman, J. Ahmad, and T. Muhammad, "Dynamics of novel exact soliton solutions to stochastic Chiral nonlinear Schrödinger equation," Alexandria Eng. J. **79**, 568–580 (2023).
[14] J. Wei, J. Y. Wang, and Y. H. Li, "Soliton and breather solutions of a reverse time nonlocal coupled nonlinear Schrödinger equation with four-wave mixing effect," Appl. Math. Lett. **157**, 109165 (2024).
[15] X. Sang, H. H. Dong, Y. Fang *et al.*, "Soliton, breather and rogue wave solutions of the nonlinear Schrödinger equation via Darboux transformation on a time-space scale," Chaos, Solitons Fractals **184**, 115052 (2024).
[16] X. Y. Luo and Y. Chen, "Darboux transformation and N-soliton solution for extended form of modified Kadomtsev–Petviashvili equation with variable-coefficient," Commun. Theor. Phys. **66**, 179–188 (2016).
[17] J. P. Wu, "N-soliton, M-breather and hybrid solutions of a time-dependent Kadomtsev–Petviashvili equation," Math. Comput. Simul. **194**, 89–96 (2022).
[18] D. J. Zhang and D. Y. Chen, "The N-soliton solutions of the sine-Gordon equation with self-consistent sources," Physica A **321**, 467–481 (2003).
[19] X. Lü and T. Geng, "Multi-soliton solutions and their interactions for the $(2+1)$-dimensional Sawada-Kotera model with truncated Painlevé expansion, Hirota bilinear method and symbolic computation," Int. J. Mod. Phys. B **23**, 5003–5015 (2009).
[20] M. H. Zhang, W. F. Weng, and Z. Y. Yan, "Interactions of fractional N-solitons with anomalous dispersions for the integrable combined fractional higher-order mKdV hierarchy," Physica D **444**, 133614 (2023).
[21] W.-X. Ma, "N-soliton solutions and the Hirota conditions in $(2+1)$-dimensions," Opt. Quantum Electron. **52**, 511 (2020).
[22] L. T. Gai and M. C. Li, "A trilinear analysis for lump-type wave, breather wave and BK-type wave solutions of a $(3+1)$-dimensional $\bar{p}$-gKP equation," Chin. J. Phys. **72**, 38–49 (2021).
[23] W.-X. Ma, "N-soliton solutions and the Hirota conditions in $(1+1)$-dimensions," Int. J. Nonlinear Sci. Numer. Simul. **23**, 123–133 (2022).
[24] Z. Q. Li, S. F. Tian, and J. J. Yang, "On the asymptotic stability of N-soliton solution for the short pulse equation with weighted Sobolev initial data," J. Differ. Equations **377**, 121–187 (2023).
[25] S. C. Mohapatra, H. Islam, T. S. Hallak, and C. G. Soares, "Solitary wave interaction with a floating pontoon based on Boussinesq model and CFD-based simulations," J. Mar. Sci. Eng. **10**, 1251 (2022).
[26] S. C. Mohapatra, R. B. Fonseca, and C. G. Soares, "Comparison of analytical and numerical simulations of long nonlinear internal solitary waves in shallow water," J. Coastal Res. **344**, 928–938 (2018).
[27] T. S. Hallak, H. Islam, S. C. Mohapatra, and C. G. Soares, "Comparing numerical and analytical solutions of solitary water waves over finite and variable depth," in ASME 40th International Conference on Ocean, Offshore and Arctic Engineering, 2021.
[28] B. B. Kadomtsev and V. I. Petviashvili, "On the stability of solitary waves in weakly dispersive media," Sovi. Phys. Dokl. **15**, 539 (1970).

[29]M. J. Ablowitz and H. Segur, "On the evolution of packets of water waves," J. Fluid Mech. **92**, 691 (1979).
[30]S. Y. Lou, "Alice-Bob systems, $\hat{P}$-$\hat{T}$-$\hat{C}$ symmetry invariant and symmetry breaking soliton solutions," J. Math. Phys. **59**, 083507 (2018).
[31]Y. L. Cao, J. S. He, and Y. Cheng, "The partial-rogue ripple solutions of nonlocal Kadomtsev–Petviashvili equation," Physica D **458**, 133990 (2024).
[32]W.-X. Ma, "Comment on the $3+1$ dimensional Kadomtsev–Petviashvili equations," Commun. Nonlinear Sci. Numer. Simul. **16**, 2663–2666 (2011).
[33]W.-X. Ma and Y. Zhou, "Lump solutions to nonlinear partial differential equations via Hirota bilinear forms," J. Differ. Equations **264**, 2633–2659 (2018).
[34]B. Ren, W.-X. Ma, and J. Yu, "Characteristics and interactions of solitary and lump waves of a $(2+1)$-dimensional coupled nonlinear partial differential equation," Nonlinear Dyn. **96**, 717–727 (2019).
[35]L. T. Gai, W.-X. Ma, and M. C. Li, "Lump-type solutions, rogue wave type solutions and periodic lump-stripe interaction phenomena to a $(3+1)$-dimensional generalized breaking soliton equation," Phys. Lett. A **384**, 126178 (2020).
[36]R. K. Alhefthi, K. U. Tariq, W.-X. Ma, and F. Mehboob, "On lump and solitonic wave structures for the $(3+1)$-dimensional nonlinear evolution model," Phys. Scr. **99**, 055223 (2024).
[37]U. K. Mandal, A. Das, and W.-X. Ma, "Integrability, breather, rogue wave, lump, lump-multi-stripe, and lump-multi-soliton solutions of a $(3+1)$-dimensional nonlinear evolution equation," Phys. Fluids **36**, 037151 (2024).
[38]X. Lü, L. L. Zhang, and W.-X. Ma, "Oceanic shallow-water description with $(2+1)$-dimensional generalized variable-coefficient Hirota–Satsuma–Ito equation: Painlevé analysis, soliton solutions, and lump solutions," Phys. Fluids **36**, 064110 (2024).
[39]L. T. Gai, W.-X. Ma, and B. Sudao, "Abundant multilayer network model solutions and bright-dark solitons for a $(3+1)$-dimensional p-gBLMP equation," Nonlinear Dyn. **106**, 867–877 (2021).
[40]L. T. Gai, Y. H. Qian, Y. P. Qin *et al.*, "Periodic bright–dark soliton, breather-like wave and rogue wave solutions to a $\bar{p}$-GBS equation in $(3+1)$-dimensions," Nonlinear Dyn. **111**, 15335–15346 (2023).
[41]L. T. Gai, W. Y. Wu, T. F. Ding *et al.*, "Lump wave solutions, lump-stripe soliton inelastic collision phenomena and rogue-type wave solutions for a generalized breaking soliton system in $(3+1)$-dimensions," Wave Motion **124**, 103243 (2024).
[42]W.-X. Ma, "Bilinear equations, Bell polynomials and linear superposition principle," J. Phys. **411**, 012021 (2013).